Journal of Process Control 121 (2023) 13–29

Contents lists available at ScienceDirect

Journal of Process Control

journal homepage: www.elsevier.com/locate/jprocont

Identifiable prediction animal model for the bi-hormonal intraperitoneal artificial pancreas

Karim Davari Benam [a,*], Hasti Khoshamadi [a], Marte Kierulf Åm [b], Øyvind Stavdahl [a], Sebastien Gros [a], Anders Lyngvi Fougner [a]

[a] Department of Engineering Cybernetics, Faculty of Information Technology and Electrical Engineering, Norwegian University of Science and Technology (NTNU), O. S. Bragstads Plass 2D, 7034 Trondheim, Norway
[b] Department of Clinical and Molecular Medicine, Faculty of Medicine and Health Sciences, Norwegian University of Science and Technology (NTNU), Erling Skjalgsons Gate 1, 7491 Trondheim, Norway

ARTICLE INFO

Article history:
Received 24 December 2021
Received in revised form 15 November 2022
Accepted 18 November 2022
Available online xxxx

Keywords:
Bi-hormonal artificial pancreas
Biological system modeling
Biological systems
Diabetes
Parameter identification

ABSTRACT

To achieve a fully automatic artificial pancreas (AP), i.e., an AP without the need for meal announcements, the intraperitoneal (IP) route is explored. This route has faster dynamics than the typical subcutaneous (SC) route. Model predictive control (MPC) is the most promising control algorithm, but it requires a predictive and identifiable model. This paper presents the design of such a model for MPC-based dual hormone IP APs. This model is trained and tested on recorded data from anesthetized pigs. Animal experiments show that the saturation of the hepatic first-pass effect is essential in how IP insulin and IP glucagon affect glucose levels. These physiological phenomena must be modeled to estimate the system behavior for various conditions. This, in turn, increases the number of parameters and complicates system identification. The availability of rich experimental data from 26 animal trials motivated the design of a technique to exploit this prior information to ensure the identifiability of our model. Through this technique, most parameters were either modeled as body weight functions or common among animals. The correlation between parameter values and body weight is discovered utilizing prior data from various animal experiments, such as blood glucose, plasma insulin, and glucagon levels, in which hormones were administered intraperitoneally or intravenously. This method simplifies the system identification for every new subject while keeping the model's essential details that improve the prediction capability relative to comparable models. The model can be exploited in MPC or any other model-based controller of a bi-hormonal IP AP. It can also be used as a simulator to develop control approaches for single and bi-hormonal IP APs.

1. Introduction

Type 1 diabetes mellitus (T1DM) is potentially a life-threatening illness in which the pancreas produces little or no insulin [1]. Frequently even glucagon production is impaired [2]. Insulin is the essential hormone to reduce blood glucose levels (BGL) by enabling cellular glucose uptake. The cells either use glucose as an energy source or store it as glycogen, e.g., the liver and skeletal muscle cells. In contrast, glucagon triggers glycogenolysis, a process that involves converting stored glycogen to glucose, releasing it into the bloodstream, and thus raising the BGL.

External insulin therapy is the current solution to control the BGL in T1DM patients. Generally, patients estimate the required amount of insulin based on their body weight, activity level, and lifestyle. Once the insulin bolus is calculated, they infuse insulin subcutaneously (SC). In an intensive care unit, it can be infused intravenously (IV), but the SC route is the standard in T1DM patients.

Nowadays, the calculations of the required insulin can be made by a device called the artificial pancreas (AP). An AP consists of an insulin pump, BGL sensors, and a control algorithm that calculates the amount of required insulin based on the patient's BGL profile and physical characteristics. The commercially available APs are discussed by Moon et al. [3] and Cobelli et al. [4].

When insulin is delivered via the IV route, as shown in Fig. 1, it is distributed throughout the body by blood circulation. Despite the quickness and reliability of the IV route, blood clots and catheter-related problems make it unsuitable for continuous insulin infusions. The SC route is safer and less invasive than the IV route [4]. Therefore, continuous subcutaneous insulin infusion (CSII) has become a widely used solution since the 1990s, and

* Corresponding author.
E-mail addresses: karim.d.benam@ntnu.no (K.D. Benam), hasti.khoshamadi@ntnu.no (H. Khoshamadi), marte.k.am@ntnu.no (M.K. Åm), oyvind.stavdahl@ntnu.no (Øy. Stavdahl), sebastien.gros@ntnu.no (S. Gros), anders.fougner@ntnu.no (A.L. Fougner).

https://doi.org/10.1016/j.jprocont.2022.11.008

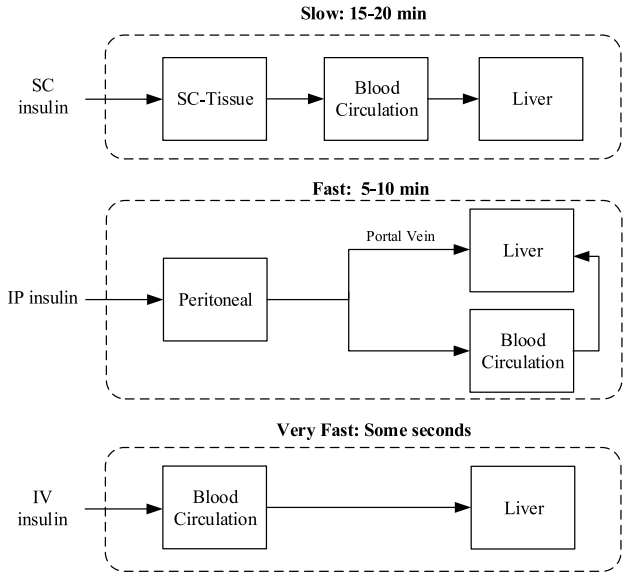

Fig. 1. Comparison of the time delays and pharmacokinetics block diagram of the SC, IP, and IV insulin administration. Notice that the HFP is saturated at greater insulin concentrations, and insulin enters the blood circulation system again by bypassing the liver.

advances in the safety and accuracy of the SC pumps and BGL sensors have improved the diabetes management.

Due to the intrinsic delay in the SC route and the slow dynamics of insulin absorption, no matter how advanced the control algorithms are, there is always a trade-off between the performance of the controllers and the risk of hypoglycemia episodes. The slow dynamics and delay can cause oscillations, especially if the control algorithm is aggressive (high gain). It requires precise control tuning to achieve a fully automated AP without meal announcement. Therefore, in commercially available single-hormonal APs, the carbohydrate content of each meal must be estimated and announced to the AP ahead of time [5].

In addition, CSII delivers insulin to the entire body in equal concentrations, whereas the primary target organ of insulin is the liver. Under normal conditions, insulin is secreted from the pancreas and transported directly to the liver via the portal vein (PV). The insulin concentration is consequently much higher in the liver than in the rest of the body. However, the non-physiological nature of CSII leads to a high concentration of insulin in peripheral tissues, which impacts the BGL control quality.

An alternative and feasible approach for delivering drugs to the liver is to deposit the drug into the peritoneal cavity [6–8]. The peritoneal cavity is a space within the abdomen enclosed by the peritoneal lining. It is lubricated by a small volume of peritoneal fluid that facilitates movements of the abdominal organs [9]. Although the peritoneal cavity is small in volume, it has a large surface area and the blood vessels within the lining, together with the blood vessels from the intestines, drain into the liver via the PV. Drug injections via this route are called intraperitoneal (IP) injections.

In addition to mimicking normal pancreatic function with IP injections, this route has significant control benefits, such as faster insulin appearance in the blood due to a higher absorption rate and also faster insulin disappearance rate due to the hepatic first-pass (HFP) effect [10]. The current challenges and solutions of using the IP route are discussed in [5].

Our recent animal studies revealed nonlinear insulin pharmacokinetics and pharmacodynamics behavior of IP route [11]. These results showed that insulin boluses of less than 0.125 U/kg rapidly affect BGL without causing a significant change in plasma insulin levels (PIL). However, despite a slight extra reduction in BGL, a substantial increase in PIL is found for greater IP insulin boluses. Unlike the IP injections, a dose-dependent relation between insulin dosage and the PIL is observed following SC administration.

These findings are consistent with saturation of the HFP effect, which holds that when insulin concentration in the PV exceeds a certain level, insulin clearance in the liver becomes saturated. As a result, more insulin enters the general blood circulation. Additionally, the insulin effect in the liver is not proportional to the size of the insulin boluses; following a large insulin bolus, the liver's capacity to absorb glucose is saturated. Therefore, the saturation of the HFP effect must be modeled to predict the body's behavior for different insulin bolus sizes.

Taking full advantage of the IP pathways in the AP systems necessitates having a mathematical model. This paper proposes a model to describe IP insulin and glucagon interaction with the BGL. The model aims to be used in APs with model-based control techniques like model predictive control (MPC). Therefore, the model should track the measured data and have a high performance in predicting future BGL. In addition, the parameters must be identifiable, and the system identification procedure must be feasible and noninvasive. It is helpful to have a short identification phase since then; one can rapidly start automated glucose management and reduce the patient involvement in glycemic control. It may be even more critical to have a short identification phase in animal experiments since it is desirable to decrease the duration of these experiments. Therefore, the model is designed with a minimum number of parameters and states necessary for mimicking the real-life behavior of the body's response to IP insulin and glucagon.

In summary, the main aim of this paper is to design a model for blood glucose prediction with IP insulin and IP glucagon with a few parameters to use in model-based control.

The proposed model extends our previous model [12] by including the HFP effect and improvement of the glucagon sensitivity sub-model. The modifications improve the model to predict the response to a wide range of insulin and glucagon boluses. In addition, to overcome the identifiability issues and ease the identification procedure, a novel method based on physiological and practical assumptions is proposed. In this method, called "meta-model identification", one could split the model's parameters into the population and individual parameters. Population parameters are a set of parameters that are functions of body weight or common among individuals/animals, and individual parameters are the parameters that vary from subject to subject. The proposed method enables us to split the invasive sets of excitation and measurements among several animal experiments instead of performing them on each animal. Notably, the population parameters are found using prior information. For every new subject, there is only a need to identify five individual parameters without an invasive excitation.

Using data from several animal experiments, we showed that the proposed model could satisfactorily reproduce the behavior of glucose metabolism in response to a wide range of insulin and glucagon boluses. Furthermore, the new model outperforms other comparable models in prediction performance, which is a crucial feature for the closed-loop performance of MPC-based methods.

The paper is structured as follows. Animal care and surgical procedures are described in Section 2, while pharmacokinetics and pharmacodynamics of insulin and glucagon are modeled in Section 3. We provide identification method and meta-model designation in Section 4. The utilized data sets and evaluation tools are described in Section 5, and the destined model is trained in Section 6. Using the test data, the performance of the proposed model in fitting to the measurements and prediction is compared with other models in Sections 7 and 8, respectively. The conclusions and discussions are provided in Section 9.

2. Methods

This section provides an overview of animal experiments and clinical procedures. The procedures are described in more detail in [11,13].

2.1. Ethical approval

The Norwegian Food Safety Authority (FOTS number 12948) approved the animal experiments, which were carried out in accordance with "The Norwegian Regulation on Animal Experimentation" and "Directive 2010/63/EU on the protection of animals used for scientific purposes".

2.2. Animals and animal handling

The tests were carried out on 29 non-diabetic farm pigs (Sus scrofa domesticus) that weighed 30–63 kg. Before the experiments, the animals were given a week to get used to the staff and their new surroundings. The animals were kept together in groups whenever possible. They were fed commercial growth feed twice a day and given unlimited water access.

2.3. Anaesthesia

The anesthesia procedure, the drugs used in this procedure, and the environmental factors are described in [11,13] in detail.

2.4. Surgical procedure

A venous line for fluid infusion was established in the left internal jugular vein, and the left carotid artery was cannulated for blood sampling and monitoring of physiological parameters. The same cut-down was used to insert both catheters. The catheters from the insulin and glucagon pumps were connected at the end and inserted 10–15 cm into the upper left part of the abdomen through a 2–3 cm long craniocaudal incision in the abdominal wall, 2–3 cm caudally to the umbilicus. The pigs were euthanized with an IV overdose of pentobarbital (minimum 100 mg/kg)(pentobarbital NAF, Apotek, Lørenskog, Norway) at the end of the experiments while fully anesthetized.

2.5. Suppression of endogenous insulin and glucagon secretion

Twenty pigs were given IV boluses of 0.4 mg octreotide (Sandostatin 200 g/ml, Novartis Europharm Limited, United Kingdom) every hour and SC injections of 0.3 mg pasireotide (Signifor 0.3 mg/ml, Novartis Europharm Limited, United Kingdom) every three hours to inhibit endogenous insulin and glucagon secretion. The remaining pigs received octreotide as a 5 g/kg/h infusion and no pasireotide injections.

2.6. Measurements

PHL was analyzed with Glucagon ELISA (10-1281-01 Mercodia, Uppsala, Sweden), and PIL was analyzed with Porcine Insulin ELISA (10-1200-01, Mercodia, Uppsala, Sweden). The assay ranges for the glucagon and porcine insulin ELISA kits were 2–172 pmol/l and 2.3–173 mU/l, respectively. Blood glucose was analyzed on a Radiometer ABL 725 blood gas analyzer (Radiometer Medical ApS, Brønshøj, Denmark).

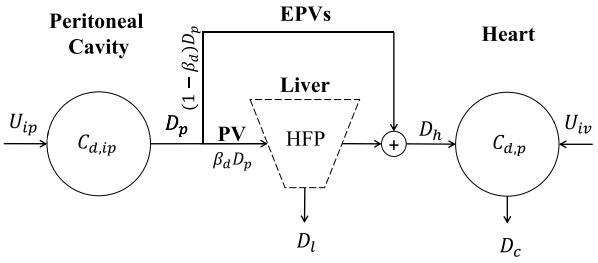

Fig. 2. Block diagram of the proposed IP drug pharmacokinetics. The IP and IV drug administration rates are denoted by U_{ip} and U_{iv}, respectively. $C_{d,ip}$ and $C_{d,p}$ are the drug concentrations in the peritoneal cavity and plasma, respectively. The portal vein (PV) and extra portal veins (EPVs) transport the drug (at a rate of D_p) from the peritoneal cavity to the liver and heart. In the liver, the drug undergoes the hepatic first-pass (HFP) effect, and a portion of it (at a rate of D_l) is removed from the blood. The remaining drug (at a rate of D_h) enters the heart and is cleared from the plasma at a rate equal to D_c.

3. Background and model development

From the pharmacokinetics point of view, drugs deposited in the IP cavity are absorbed by the surrounding capillaries and transported to other organs via blood circulation [14]. The capillaries in the vicinity of the peritoneum can be divided into two groups, (a) capillaries emptying compounds into the PV and (b) capillaries draining into the extra-portal veins (EPVs). The PV carries blood from the stomach, intestines, spleen, and pancreas to the liver and is essential in transferring insulin and glucagon from the pancreas to the liver in the body. The EPVs go directly to the heart. Notably, drugs absorbed into the PV and transported to the liver are subject to the HFP effect, and a significant portion is cleared from the blood before reaching the systemic circulation.

From the pharmacodynamics point of view, the liver can store glucose as glycogen in quantities of up to 6% of its weight, which equates to 100–120 g glycogen for a 70 kg male. Other organs, such as skeletal muscles, kidneys, and lungs, may not substantially influence the BGL, but their cumulative impact is comparable to that of the liver. For example, skeletal muscle glycogen storage can amount to 2% of their weight, allowing for a total of 400 g of glycogen storage in the muscles of the body as a whole [15,16]. Therefore, the liver and other organs' cumulative pharmacodynamics must be modeled separately to describe the effect of insulin.

In the following sections, the mathematical models of the pharmacokinetics and pharmacodynamics of insulin and glucagon are described.

3.1. IP insulin and glucagon pharmacokinetics

To simulate the pharmacokinetics of insulin and glucagon in the body, one should model the concentration dynamics of these drugs in peritoneal fluid, the quantity of the drugs entering the liver and the heart, and the concentration of the drug in plasma. The equations are given in the following sections, and the block diagram of the proposed IP pharmacokinetics is presented in Fig. 2.

3.1.1. Concentration of the drugs in peritoneal fluid

The IP cavity fluid is where the drugs are administrated, and drug dissemination relies on its dynamics. Similarly to Canal et al. [17] and Zazueta et al. [12], we modeled the concentration of the drugs (i.e., insulin or glucagon) in the peritoneal cavity as a linear system as follows:

$$\dot{C}_{d,ip} = -k_{d_1} \cdot C_{d,ip} + \frac{U_{ip}}{V_{d,ip}} \tag{1}$$

where $C_{d,ip}$ [mass/ml] is the concentration of drugs in the peritoneal fluid, U_{ip} [mass/min] is the mass rate of drug injection, $V_{d,ip}$ [ml] is the volume of the peritoneal fluid, and k_{d_1} [min^{-1}] is the diffusion rate of the drug from the peritoneal cavity to capillaries. From (1) one can conclude that

$$D_p \triangleq k_{d_1} V_{d,ip} C_{d,ip} \tag{2}$$

is the rate at which the mass of a drug escapes from the peritoneal cavity and gets absorbed into the capillaries that surround the peritoneal cavity.

3.1.2. Mass rate of drug entering to liver

A sizeable portion of D_p eventually drains into the PV, and the rest goes to the heart via EPVs [14]. As shown in Fig. 2, the PV supplies blood from the abdominal organs to the liver, where the main metabolism of glucose takes place. The drug mass rate entering the PV can be defined as $\beta_d D_p$ where $0 < \beta_d \leq 1$ is the ratio of drug drained into the PV to the total amount of drug that is absorbed from the peritoneal cavity.

Notably, the HFP effect becomes saturated for a high IP insulin bolus, and the liver cannot remove the drug from the blood in the PV. We used the model suggested in [18] to model the hepatic drug clearance rate and its saturation as follows.

$$D_l = k_{d_2} \frac{\beta_d D_p}{k_{d_3} + \beta_d D_p} \tag{3}$$

where D_l is the liver clearance rate, k_{d_2} [mass/min] is the maximum drug clearance rate of the liver, and k_{d_3} [mass/min] is the half-saturation constant in the liver response function [19].

3.1.3. Mass rate of drugs entering to heart

The drug bypassing the HFP effect or absorbed into the EPVs will ultimately reach the heart and spread throughout the body. Therefore, the drug mass rate entering the heart, D_h, can be found as follows.

$$D_h = D_p - D_l \tag{4}$$

3.1.4. Concentration of drugs in plasma

The quantity of drugs available to the different tissues in the body is dissolved in blood plasma. In addition, the concentration of the drug in the blood is a measurable quantity modeled as follows in this paper.

$$\dot{C}_{d,p} = -k_{d4} C_{d,p} + (U_{iv} + D_h)/V_{d,p} \tag{5}$$

where $C_{d,p}$ is the concentration of drugs in plasma [mass/l], U_{iv} is IV drug infusion rate [mass/min], and k_{d4} is the clearance rate of the drug from plasma [min^{-1}], and $V_{d,p}$ is the volume of the plasma that the drug is solved in [l]. Notably, $D_c \triangleq V_{d,p} k_{d4} C_{d,p}$ is the drug mass clearance rate from plasma [mass/min].

Please note that peritoneal fluid in people ranges from 50 to 75 ml [20], whereas a 70 kg man's blood volume is 5.81 l [21]. In order to avoid showing low values for $V_{d,ip}$, or large values for blood volume, we choose to measure $V_{d,ip}$ in milliliters and the blood volumes in liters.

3.1.5. Summary of the proposed pharmacokinetics model

In summary, a general model for the pharmacokinetics of IP and IV administrations is developed. For insulin and glucagon injections, one needs to replace d with {i: insulin, and h: glucagon} in the notations. The unit [mass] must also change with [U] and [μg] for insulin and glucagon, respectively. Notably, mg is the most common unit for glucagon. However, in our animal experiments, due to the size of the pigs, glucagon injection doses were mainly in the range of 0 to 150 μg. Therefore, μg is chosen as the mass unit for the glucagon in this paper.

The block diagram and the equations are summarized in Figs. 2 and 3. In the next section, the effects of both insulin and glucagon on BGL are modeled using the proposed pharmacokinetics model.

3.2. IP insulin and glucagon pharmacodynamics

The purpose of this section is to model the reaction of the organs receiving insulin and glucagon.

3.2.1. Effective insulin in liver

In this study, it is assumed that the rate of glucose absorption in the liver is proportional to the quantity of insulin taken up by the liver cells. The liver will then take up glucose based on the insulin sensitivity of the cells and the amount of glucose in the blood. For the sake of simplicity, the amount of insulin taken up by the liver cells is called effective insulin.

To develop a mathematical model for the effective insulin rate in the liver, we assume it is a linear system that responds to the rate at which the liver absorbs insulin from the PV. Since there is a saturation in the insulin uptake from the PV, the effective insulin in the liver will also be saturated for higher amounts of insulin. Therefore, using (1) and the HFP saturation (see Eq. (3)), the concentrations of insulin in the IP cavity and the effective insulin in the liver are modeled as follows:

$$\dot{E}_{i,l} = \frac{1}{\tau_l}\left(-E_{i,l} + k_{i_2} \frac{\beta_i V_{i,ip} k_{i_1} C_{i,ip}}{k_{i_3} + \beta_i V_{i,ip} k_{i_1} C_{i,ip}}\right) \tag{6}$$

$$\dot{C}_{i,ip} = -k_{i_1} C_{i,ip} + \frac{I}{V_{i,ip}} \tag{7}$$

where $E_{i,l}$ is the effective insulin rate in the liver [U/min], $C_{i,ip}$ is the concentration of insulin in the peritoneal fluid [U/ml]. τ_l is the liver response time to insulin [min], and I is the rate of insulin infusion into the peritoneal cavity [U/min]. In addition, k_{i_1}, k_{i_2} and k_{i_3} are diffusion rates of the drug from the peritoneal cavity to capillaries [min^{-1}], maximum insulin clearance rate of the liver from blood [U/min], and half-saturation of the insulin HFP effect [U/min], respectively.

3.2.2. Effective insulin in the extra hepatic organs

The amount of insulin that reaches the heart is distributed throughout the systemic circulation and to the other organs. For a model developed for control purposes, describing the insulin action in each of these organs is not advisable since it introduces more parameters to the model. Therefore, this paper modeled the cumulative effective insulin in body organs (other than the liver), where effective insulin in body organs is the amount of insulin absorbed by the insulin receptors.

$$\dot{E}_{i,b} = \frac{1}{\tau_b}\left[-E_{i,b} + \left(V_{i,ip} k_{i_1} - k_{i_2} \frac{\beta_i V_{i,ip} k_{i_1}}{k_{i_3} + \beta_i V_{i,ip} k_{i_1} C_{i,ip}}\right) C_{i,ip}\right] \tag{8}$$

where $E_{i,b}$ is the effective insulin rate in the body organs other than the liver [U/min] and τ_b is the body response time to insulin [min].

3.2.3. Effective glucagon

Similar to the insulin sub-model, the effective glucagon in the liver is defined as the number of cells allowed by glucagon to break down glycogen. Notably, the amount of released glucose depends not only on the number of cells receiving glucagon but also on the amount of glycogen stored mainly in the liver or possibly other organs. The cumulative effective glucagon is only considered in the liver to simplify the model and reduce the number of parameters. Additionally, to account for unmodeled glycogenolysis in other organs, we assume that the liver is a linear system that responds proportionally to the amount of glucagon

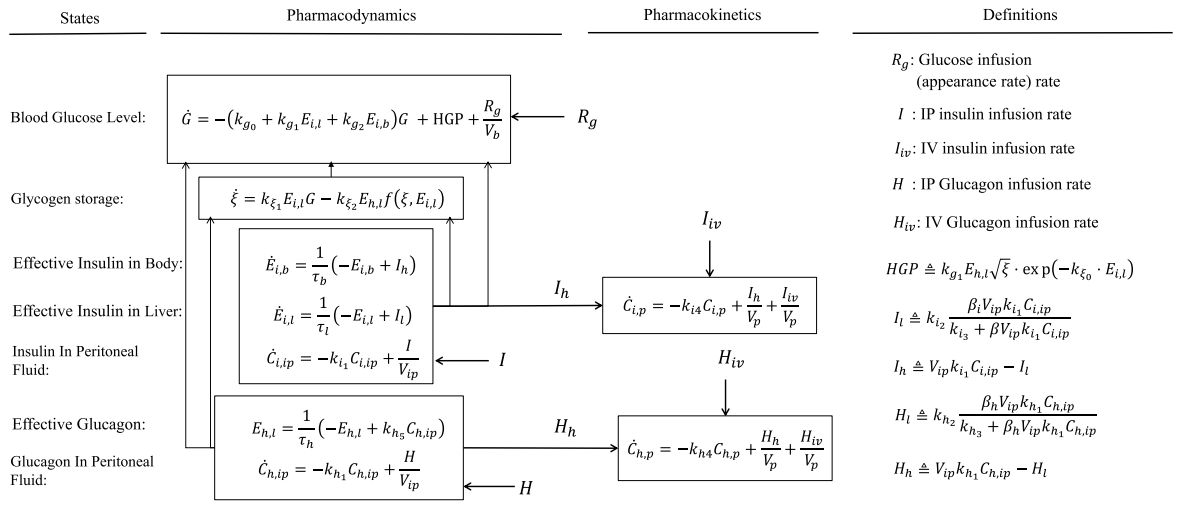

Fig. 3. Diagram and equations summary of the proposed model. In this model, inputs are IP insulin (I), IP glucagon (H), IV insulin (I_{iv}), and IV glucagon (H_{iv}). Outputs of the model are blood glucose level (G), the concentration of insulin in plasma ($C_{i,p}$), and the concentration of glucagon in plasma ($C_{h,p}$). In addition, $E_{d,j}$ are the effective drug ($d \in \{i : \text{insulin}, h : \text{glucagon}\}$) in the compartments $j \in \{l : \text{liver}, b : \text{body organs}\}$. Moreover, ξ is the glycogen storage level. The rest of the variables are the constant parameters defined in Section 3.

absorbed from the peritoneal cavity without taking the HFP effect into account. The effective glucagon rate is modeled as follows:

$$\dot{E}_{h,l} = \frac{1}{\tau_h}\left(-E_{h,l} + k_{h_5}C_{h,ip}\right) \tag{9}$$

$$\dot{C}_{h,ip} = -k_{h_1}C_{h,ip} + \frac{H}{V_{h,ip}} \tag{10}$$

where H is the rate of IP glucagon infusion [μg/min], $C_{h,ip}$ is the concentration of glucagon in the peritoneal fluid [μg/ml], $E_{h,l}$ is the effective glucagon rate in the liver [μg/min]. Parameters k_{h_1} and τ_h are, respectively, the glucagon diffusion rate from the peritoneal cavity to the capillaries [min^{-1}] and the response time of the body to glucagon [min]. Furthermore, k_{h_5} is a constant parameter [ml/min].

3.2.4. Mathematical model for hepatic glucose production rate

Glycogenolysis is the liver's process of producing glucose in response to effective glucagon. The experiments showed that the amount of glucose produced depends on the effective glucagon, insulin, and glycogen stored in the liver.

According to the literature, glycogen is predominantly stored in the cytoplasm of hepatocytes. Zazueta et al. [12] described glycogenolysis sensitivity to glycogen storage level as a linear function. Notably, a high glycogen storage level does not necessarily result in increased glucose production because the glucagon may not diffuse to all liver cells simultaneously, and the liver's glycogenolysis rate can be subjected to saturation. In addition, one can assume that having insulin in the liver decreases glycogenolysis. To account for these assumptions, we define the hepatic glucose production rate as follows.

$$HGP \triangleq k_{g_3} \cdot E_{h,l} \cdot \sqrt{\xi} \cdot \exp\left(-k_{\xi_0} \cdot E_{i,l}\right) \tag{11}$$

where HPG [mmol/l/min] is the hepatic glucose production rate, $\xi \in [0 - 100]\%$ is liver glycogen storage level modeled as described in (12). The term $\sqrt{\xi}$ refers to the saturation of the liver in terms of glucose production, k_{ξ_0} [min/U] is a constant parameter describing the negative influence of effective insulin rate in the liver on glucose production rate, and k_{g_3} is a coefficient describing the sensitivity of liver cells to effective glucagon in the liver, glycogen storage level, and effective insulin in the liver [$\frac{mmol}{l \cdot \sqrt{\%} \cdot \mu g}$].

3.2.5. Glycogen storage level

We assume that glucose absorbed by the liver is stored as glycogen and thus increases glycogen storage level, whereas hepatic glucose production decreases glycogen storage level. With these assumptions and using (13), one can model the dynamics of the liver glycogen storage level for $\xi(t_0) \in [0, 100]\%$ as follows.

$$\dot{\xi} = \begin{cases} k_{\xi_1}\, E_{i,l}\, G - \frac{k_{\xi_2}}{k_{g_3}} HGP & \xi \in [0, 100]\% \\ 0 & \text{otherwise} \end{cases} \tag{12}$$

where k_{ξ_1} [%· l/mmol/U] and k_{ξ_2} [$\sqrt{\%}/\mu$g] are constant values representing the charging and discharging rates of the glycogen storage. One can assume that these parameters are proportional to the weight of the liver. In addition, G is BGL defined in (13). Notably, the term $k_{\xi_1}E_{i,l}G$ is proportional to the rate of glucose that liver uptakes.

3.3. Blood glucose dynamics

Using the proposed sub-models for insulin and glucagon in the body, it is now possible to model the aggregated effect of insulin and glucagon on the BGL. To achieve this, we employed the following equation.

$$\dot{G} = -\left(k_{g_0} + k_{g_1} \cdot E_{i,l} + k_{g_2} \cdot E_{i,b}\right) \cdot G + HGP + R_g(t)/V_b \tag{13}$$

where G is the blood glucose level [mmol/l]. $R_g(t)$ is the glucose appearance rate due to meal digestion [mmol/min], and V_b [l] is the volume of the blood circulating in the body. k_{g_0} is the insulin-independent glucose uptake rate [min^{-1}] (e.g., brain glucose uptake rate). k_{g_1}, and k_{g_2} are the sensitivity rates of the subjects to effective insulin in liver [U^{-1}], and in the organs other than liver [U^{-1}], respectively.

3.4. Summary of model development

An overview of the proposed mathematical model of the pharmacokinetics and pharmacodynamics for both IP insulin and glucagon infusions is shown in Fig. 3. The challenges of the parameter identification for the proposed model are explored in the next section.

4. Practical techniques to ensure identifiability and reduce the time needed to identify the parameters

In order to use the model for control purposes, we must ensure that the parameters of the model are identifiable in two ways:

1. **Structural identifiability**: The necessary condition for having structurally identifiable parameters is to have no redundant parameters in the model. Otherwise, there will be a set of parameters that may vary without changing the output. Therefore, the parameters are not uniquely identified [22].
2. **Practical identifiability:** The data used to estimate the parameters provides sufficient information, making it practically possible to identify them. The amount of data required for a reliable estimation of the parameters typically increases with the number of parameters. In addition to the amount of data, we must ensure that the inputs are rich enough to excite the system dynamics [22]. For example, different insulin bolus sizes must be injected to capture the dynamics of the HFP and the insulin pharmacodynamics.

It is worth highlighting that, from a control perspective, the short identification tests and the procedures are desirable because one can start the closed-loop system shortly. However, To excite all the system dynamics in a short time window, one needs extreme inputs, which can be dangerous and invasive.

One solution to increase the identifiability and shorten the identification phase is to embed prior physiological knowledge in the parameter identification process. For example, the model is based on body physiology and drug concentrations in compartments; some parameters strongly correlate to the compartment volume and the body weight. Therefore, we can use past data from different animals to estimate these relationships and embed them in the system identification procedure.

In addition, an easy step in addressing the structural non-identifiability issue is to model additional physical quantities that can be measured. PIL and PHL are two physical quantities that can be measured by taking blood samples and analyzing them in laboratories. However, these measurements are not real-time.

One can use the PIL and PHL measurements to find the parameters correlated to body weight or constant across the subjects in a post-processing manner. For simplicity, one can assume that the observed correlation between body weight and the selected parameters applies generally, and one can extrapolate from these data to all subjects.

Additionally, by combining the PIL and PHL measures with the IV injections, it may be possible to increase identifiability. This is achievable because adding the IV injections to the identification procedure results in a new map from a new input to states while maintaining the original mapping of states to outputs. Consequently, it can increase structural identifiability [22].

Another way to improve identifiability is to use the literature to find the values for the parameters based on the body's physiology. For example, V_b can be estimated using body weight, and gender [23,24]. These assumptions and information can help improve the model's practical and structural identifiability.

In summary, the following ideas are used in this study to solve the identifiability issues of the proposed model:

1. Perform specific experiments with frequent PIL and PHL measurements to improve the structural identifiability.
2. Perform specific experiments with IV insulin and glucagon boluses to excite dynamics in an efficient way.
3. Find the parameters that are dependent on body weight or are almost constant among subjects.
4. If available, look up the values of the physiology-based parameters in the literature.

In order to find the parameters that have the same values among the subjects or are correlated with body weight, a general model is needed to simulate several subjects together. To put the above concepts into action and analyze the information of different animals, we introduced the "meta-model". It is a generic model that allows us to examine a group of animals (subjects) linked by constant and weight-dependent parameters. Adding other features, such as gender, can also improve the model, but we did not include other features in this study. The meta-model is introduced in the next section.

4.1. Meta-model development

This section aims to expand the suggested model (summarized in Fig. 3) to simulate subjects in a population who share parameters related to body weight or that are constant across the population in order to apply the concepts discussed in the previous section. To this end, we categorize the parameters of the proposed model into four groups:

1. **Independent parameter:** A set of parameters that must be identified for each animal (subjects) separately. In this paper, we assumed that the initial values of the states $\{x_1, \dots, x_7, z_1, z_2\}$ in Eqs. (14b) and (14a) belong to this set, and they are denoted by $\mathbf{A} \triangleq \{\alpha_1, \alpha_2, \dots, \alpha_9\}$. Notably, among parameters, α_7 has an essential role in the model since it is the initial glycogen storage level.
2. **Analogous parameters:** A set of parameters which consist of values similar across individuals. However, they must be identified individually, e.g., see the parameters in Eqs. (14a)–(14e) that are noted by $\mathbf{B} \triangleq \{\beta_1, \beta_2, \dots \beta_{19}\}$.
3. **Weight-dependent parameters:** A set of parameters that depends on body weight. This parameter set is defined as $\mathbf{\Gamma} \triangleq \{\gamma_1, \gamma_2, \dots, \gamma_9\}$ in the Eqs. (16) and (17).
4. **Constant parameters:** A set of parameters that have the same value for all animals in normal situations, e.g., see the parameters denoted by $\mathbf{\Delta} \triangleq \{\delta_1, \delta_2, \dots, \delta_{15}\}$ in the Eqs. (16), (17), (14d), and (14e).

Using categories for the parameter sets described above, and the proposed model summarized in Fig. 3, a meta-model is introduced in (14a) and (14b) where the detailed comparison with the individual model is given in Table 1. Notably, $X \triangleq [G, A_{i,b}, A_{i,l}, C_{i,ip}, A_{h,l}, C_{h,ip}, \xi]^T$ is a vector including the necessary states for model base controllers. The state vector $Z \triangleq [C_{i,p}, C_{h,p}]^T$ contains the model of insulin and glucagon pharmacokinetics in the plasma. The model (14b) does not rely on the states of (14a) while it provides necessary information for controllers. Therefore, one may not consider (14a) in the controller (depending on how the complexity of the controller). However, using it in the identification can increase the identifiability of the (14b) because the two models share parameters and (14a) add two new measurable variables.

$$\frac{d}{dt}\begin{pmatrix} z_1 \\ z_2 \end{pmatrix} = \begin{pmatrix} -\beta_{12} z_1 + \beta_{13}\left(\gamma_5(\omega)\cdot x_4 - F_{sat}\right) \\ -\beta_{14} z_2 + \beta_{15}\left(\gamma_6(\omega)\cdot x_6 - F_{sat}\right) \end{pmatrix} + \frac{1}{\omega}\begin{pmatrix} \beta_{18}\cdot I_{iv}(t) \\ \beta_{19}\cdot H_{iv}(t) \end{pmatrix} \tag{14a}$$

Table 1
Description of the states, inputs and parameters of the proposed meta-model (14b).

States	Units	Description
x_1	mmol/L	Blood Glucose Level (G)
x_2	U/min	Effective Insulin in Body ($E_{i,b}$)
x_3	U/min	Effective Insulin in Liver ($E_{i,l}$)
x_4	U/mL	Insulin in IP fluid ($C_{i,ip}$)
x_5	µg/min	Effective Glucagon in Body ($E_{h,l}$)
x_6	µg/mL	Glucagon in IP Fluid ($C_{i,ip}$)
x_7	%	Glycogen storage Level (ξ)
z_1	U/L	Insulin in Plasma ($C_{i,p}$)
z_2	µg/L	Glucagon in Plasma ($C_{h,p}$)
Inputs		
R_g	mmol/min	IV Glucose Infusion rate
$I(t)$	U/min	IP Insulin rate$^{(*)}$
$I_{iv}(t)$	U/min	IV Insulin rate$^{(*)}$
$H(t)$	µg/min	IP Glucagon rate$^{(*)}$
$H_{iv}(t)$	µg/min	IV Glucagon rate$^{(*)}$
Parameters		**Equivalent to:**
ω, ω_0	kg	body weight, See Eq. (16)
β_1	min^{-1}	k_{g_0}
β_2, β_3	U^{-1}	k_{g_1}, k_{g_2}
β_4	mmol/L/µg	k_{g_3}
β_5, β_8, β_9	min^{-1}	${\tau_b}^{-1}$, ${\tau_l}^{-1}$, ${\tau_h}^{-1}$
β_6, δ_{13}	U/min	k_{i_2}, k_{i_3}
β_7, β_{10}	1/mL, mL/min	$V_{i,ip}^{-1}$, k_{h_5}
β_{11}	Dimensionless	k_{ξ_0}
β_{12}, β_{14},	min^{-1}	k_{i_4}, k_{h_4}
β_{13}, β_{15}	L^{-1}	See Eq. (16)
β_{16}, β_{17}	µg/min, 1/mL	k_{h_2}, ${V_{h,ip}}^{-1}$
β_{18}/ω, β_{19}/ω	L^{-1}	${V_{h,p}}^{-1}$, ${V_{i,p}}^{-1}$
δ_1, δ_4, δ_7	–$^{(**)}$	See Eq. (17)
$\delta_{2,3,5,6,8-11}$	–$^{(**)}$	See Eq. (16)
δ_{12}, δ_{14}	Dimensionless	β_i, β_h
$\delta_{13,15}$	U/mL, µ/mL	k_{i_3}, k_{h_3}
α_7	$[0-100]\%$	$\xi(0)$

$^{(*)}$ For simplicity, we assumed the insulin and glucagon boluses were given over 5 minute regardless of bolus size.
$^{(**)}$ According to the given equations.

$$\frac{d}{dt}\begin{pmatrix} x_1 \\ x_2 \\ x_3 \\ x_4 \\ x_5 \\ x_6 \\ x_7 \end{pmatrix} = \begin{pmatrix} -(\beta_1+\beta_2\cdot x_2+\beta_3\cdot x_3)\cdot x_1 + HGP_{meta} \\ \beta_5\,(-x_2+(\beta_7\cdot\gamma_1(\omega)\cdot x_4 - F_{sat})) \\ \beta_8\,(-x_3+F_{sat}) \\ -\gamma_1(\omega)\cdot x_4 \\ \beta_9\,(-x_5+\beta_{10}x_6) \\ -\gamma_2(\omega)\cdot x_6 \\ \gamma_3(\omega)\cdot x_3\cdot x_1 - \gamma_4(\omega)\cdot x_5\cdot HFP_{meta}/\beta_4 \end{pmatrix} + \begin{pmatrix} \gamma_7(\omega)R_g(t) \\ 0 \\ 0 \\ \gamma_8(\omega)I(t) \\ 0 \\ \gamma_9(\omega)H(t) \\ 0 \end{pmatrix} \tag{14b}$$

$$HGP_{meta} \triangleq \beta_4 x_5\sqrt{x_7}\cdot\exp\left(-\beta_{11}\cdot x_3\right), \tag{14c}$$

$$F_{sat}(x_4) \triangleq \beta_6\frac{\delta_{12}\gamma_5(\omega)x_4}{\delta_{13}+\delta_{12}\beta_7\gamma_1(\omega)x_4}, \tag{14d}$$

$$\bar{F}_{sat}(x_6) \triangleq \beta_{16}\frac{\delta_{14}\gamma_6(\omega)x_6}{\delta_{15}+\delta_{14}\beta_{17}\gamma_2(\omega)x_6} \tag{14e}$$

In summary, the measurable outputs of the introduced meta-model are:

$$\begin{cases} y_1 \triangleq x_1, & \text{blood glucose level (BGL)} \\ y_2 \triangleq z_1, & \text{plasma insulin level (PIL)} \\ y_3 \triangleq z_2, & \text{plasma glucagon level (PHL)} \end{cases} \tag{15}$$

Here y_1 is measured from all animal experiments, while y_2 and y_3 are available from some experiments. Furthermore, (14d) and (14e) are insulin and glucagon HFP effect saturation functions. Notably, we assume that the weight-dependent parameters are as follows:

$$\begin{cases} \gamma_1(\omega) \triangleq \delta_2\cdot(1+\delta_3\cdot f_\omega(\omega)) \\ \gamma_2(\omega) \triangleq \delta_5\cdot(1+\delta_6\cdot f_\omega(\omega)) \\ \gamma_3(\omega) \triangleq \delta_8\cdot(1+\delta_9\cdot f_\omega(\omega)) \\ \gamma_4(\omega) \triangleq \delta_{10}\cdot(1+\delta_{11}\cdot f_\omega(\omega)) \\ \gamma_5(\omega) \triangleq \beta_7\cdot\delta_2\cdot(1+\delta_3\cdot f_\omega(\omega)) \\ \gamma_6(\omega) \triangleq \beta_{17}\cdot\delta_5\cdot(1+\delta_6\cdot f_\omega(\omega)) \end{cases} \tag{16}$$

where $f_\omega(\omega) \triangleq (\omega/\omega_0 - 1)$ is the function describing the effect of body weight on the parameters, ω is body weight, and ω_0 is the maximum body weight among the subjects, e.g., we chose $\omega_0 = 52$ kg, which is the body weight of the Pig#6 since it was the heaviest pig in our IP experiments.

In Eq. (16), γ_1 [min^{-1}] and γ_2 [min^{-1}] are the diffusion rates of insulin and glucagon from the peritoneal cavity to the surrounding capillaries (equivalent to k_{i_1} and k_{h_1} introduced in Section 3.1.1), respectively. Since the size of the IP cavity varies with body weight, γ_1 and γ_2 are considered functions of ω. Moreover, γ_3 [% l/mmol/U] and γ_4 [% l/mmol/μg] are the charging and discharging rate of glycogen storage level (equivalent to k_{ξ_1} and k_{ξ_2} introduced in Section 3.2.5), respectively. Since the liver size is related to body weight, we assumed that γ_3 and γ_4 are weight-related parameters.

IV glucose infusion was used in the experiments to simulate meal absorption in the anesthetized pigs. The glucose solution had a concentration of 200 mg/ml. Therefore, $\gamma_5(\omega)$ is a coefficient directly related to the concentration of IV glucose infusion and inverse to the body weight (blood volume). In addition, $\gamma_6(\omega)^{-1}$, and $\gamma_7(\omega)^{-1}$ are the volumes of peritoneal fluid in which insulin and glucagon are dissolved. These parameters are defined as follows:

$$\begin{cases} \gamma_7(\omega) \triangleq \frac{\delta_1}{\omega}, \quad \gamma_8(\omega) \triangleq \frac{\delta_4}{\omega} \\ \gamma_9(\omega) \triangleq \frac{\delta_7}{\omega} \end{cases} \tag{17}$$

4.2. Parameter identification

In the animal trials, we assume that the endogenous insulin and glucagon are negligible, and we know there were no IP insulin or glucagon boluses before the experiments. Therefore, the initial values of the states $x_2, x_3, \ldots, x_6$ are zero (i.e., the values of $\alpha_2, \ldots, \alpha_6$ are zero). Moreover, α_1, α_8, and α_9 are chosen equal to BGL, PIL, and PHL measurements at $t = 0$. The initial glycogen storage is a function of different factors, and therefore α_7 needs to be identified individually. In addition, the weight-dependent parameters (Γ) are designed as body weight functions and constant parameters across the animals. Therefore, we only need to identify $\Theta \triangleq \{\beta_1, \beta_2, \ldots, \beta_{19}, \alpha_7\}$ which are individual parameters and $\Delta \triangleq \{\delta_1, \delta_2 \ldots, \delta_{15}\}$ that are constant parameters across the animals. As previously stated, we expect the individual parameters (except the initial values) of different pigs to be in the same range with a slight variation due to their similar properties.

Objective function (18) is designed for trajectory-fitting and parameter identification. Using the proposed objective function, the modeled BGL, PIL, and PHL tried to fit the measurements in N animals. Each pig is allowed to have individual parameters, but the objective function contains a penalty on the variation of these

parameters across animals. The designed objective function is as follows.

$$J(\Theta_1, \Theta_2, \ldots, \Theta_N, \Delta) = \sum_{i=1}^{N} \Big(E_{G_i}(\Theta_i, \Delta)^T \cdot Q_{G_i} \cdot E_{G_i}(\Theta_i, \Delta) + E_{I_i}(\Theta_i, \Delta)^T \cdot Q_{I_i} \cdot E_{I_i}(\Theta_i, \Delta) + E_{H_i}(\Theta_i, \Delta)^T \cdot Q_{H_i} \cdot E_{H_i}(\Theta_i, \Delta) + (\Theta_i - \bar{\Theta})^T \cdot Q_\theta \cdot (\Theta_i - \bar{\Theta}) \Big) \quad (18)$$

where:

- $E_{G_i}(\Theta_i, \Gamma)$, $E_{I_i}(\Theta_i, \Gamma)$ and $E_{H_i}(\Theta_i, \Gamma)$ are the fitting error vectors of the model in tracking the BGL, PIL and PHL measurements, respectively. They are defined as the following:

$$E_{G_i}(\Theta_i, \Delta) \triangleq \begin{pmatrix} \mathrm{BGL}_i(t_0) - y_1(\Theta_i, \Delta, t_0) \\ \mathrm{BGL}_i(t_1) - y_1(\Theta_i, \Delta, t_1) \\ \vdots \\ \mathrm{BGL}_i(t_{n_i}) - y_1(\Theta_i, \Delta, t_{n_i}) \end{pmatrix}, \quad (19)$$

$$E_{I_i}(\Theta_i, \Delta) \triangleq \begin{pmatrix} \mathrm{PIL}_i(t_0) - y_2(\Theta_i, \Delta, t_0) \\ \mathrm{PIL}_i(t_1) - y_2(\Theta_i, \Delta, t_1) \\ \vdots \\ \mathrm{PIL}_i(t_{n_i}) - y_2(\Theta_i, \Delta, t_{n_i}) \end{pmatrix}, \quad (20)$$

and

$$E_{H_i}(\Theta_i, \Delta) \triangleq \begin{pmatrix} \mathrm{PHL}_i(t_0) - y_3(\Theta_i, \Delta, t_0) \\ \mathrm{PHL}_i(t_1) - y_3(\Theta_i, \Delta, t_1) \\ \vdots \\ \mathrm{PHL}_i(t_{n_i}) - y_3(\Theta_i, \Delta, t_{n_i}) \end{pmatrix}. \quad (21)$$

- $\bar{\Theta}$ is the vector of the average individual parameters identified for the test data:

$$\bar{\Theta} = (\Theta_1 + \Theta_2 + \cdots + \Theta_N)/N. \quad (22)$$

- Q_{G_i}, Q_{I_i}, and Q_{H_i} are positive definite matrices that should be chosen according to the variance of the measurement noise and the scale of the measurements. Matrix Q_θ is also positive definite and should be chosen according to the expected variability of each parameter. For the animals or the samples that the PIL and PHL are not available, both $E_{I_i}(\Theta_i, \Gamma)$ and $E_{H_i}(\Theta_i, \Gamma)$ are zero.

4.3. Summary of the proposed identification method

In order to address the practical identifiability issues, we propose a meta-model that can characterize some parameters as either function of body weight or as constant among all animals.

To address the structural non-identifiability, we added PIL and PHL measurements as new outputs and IV drug injections as new inputs to the meta-model. However, measuring the BGL, PIL, and PHL necessitates at least 1–1.5 ml of blood to be extracted at each sampling time, which can interfere with the normal glucose metabolism of the animals. Therefore, due to animal safety, we cannot measure the PIL and PHL in all animals.

Notably, some analogous parameters can have a negligible variation among animals and, therefore, can be considered a constant parameter. In order to find these parameters, the following steps are done in the following sections:

1. Choose training data and test data.
2. Identify the parameters belonging to the sets Δ and Θ for training data.
3. Analyze the analogous parameters to find more parameters that can be considered fixed among the animals using the sensitivity and inter-subject coefficient of variability.
4. Re-identify the remaining parameters and evaluate the model by assuming the fixed parameters are known.
5. Compare the meta-model with other models for test and training data sets.

5. Training data, test data, and evaluation methods

Data collected in 26 animal experiments are used to evaluate the performance of the proposed model and identification method. Experiments are numbered Pig #1–29. Pigs #19–21 received SC insulin injections, which are outside the scope of this paper and were excluded from this analysis. Pigs #1–10 are bi-hormonal IP experiments, Pigs #11–14 are bi-hormonal IP experiments with additional IV boluses, and the rest contain only IP insulin injections. The durations of the experiments are 420–725 min, except Pig #15, which lasted only 250 minutes. BGL was measured every five minutes. In other words, the number of samples for the experiments are 84–145 samples, and 50 samples in Pig #15.

A set of 13 experiments is selected as training data to estimate the parameters of the proposed meta-model and verify its performance, while the remaining 13 experiments are considered test data. Each group of experiments chosen for training has a specific purpose in the identification, to ensure that all dynamics are excited. Table 2 describes experiment IDs, characteristics, and key features of the selected experiments. Group 1 helps to excite the dynamics of insulin, glucagon sub-models, and glycogen storage level. Group 2 helps in the identification of parameters related to body weight and the excitation of insulin and glucagon pharmacokinetics. Group 3 helps to excite the dynamics of the HFP effect since they include a wide range of insulin boluses.

Among the selected experiments, we used BGL measurements of {Pigs #2, 4, 5, 6, 10, 15, 22, 23}, PIL measurements of {Pigs #4, 5, 6, 11, 12, 13, 22, 23}, and PHL measurements of {Pigs #4–7, 11–14} for identifying the parameters of the BGL, PIL and PHL sub-models, respectively.

Notably, to estimate the parameters of (14b), one needs to ensure that the dynamics of all compartments are excited. To this end, we performed four specific experiments, which are Pigs #11–14. In these experiments, we excited the glycogen storage dynamics by injecting insulin and glucagon in different combinations. In addition, IV insulin and glucagon were also infused. The body weight of the pigs used in these experiments was chosen in the range of 30–63 kg to increase the identifiability of the body weight-related parameters.

5.1. Parameter coefficient of variability

After the identification using the training data set, the estimated analogous parameters will be analyzed to find the inter-subject parameter variability. This will be used to find the parameters that can be considered as constant across the animals. To this end, the coefficient of variability (CV_p) for parameters and sensitivity of the outputs to a parameter ($S_p^{y_i}$) are defined as follows:

$$CV_p = \frac{p - \bar{p}}{\bar{p}} 100\% \quad (23)$$

$$S_p^{y_i} = \frac{\partial y_i}{\partial p} \cdot \frac{p}{y_i}\Big|_{p=p^*} \forall i = \{1, 2, 3\} \quad (24)$$

where p^* is the estimated value of the parameter p, $\bar{p}$ is the average value of that parameter identified for the training experiments, and y_i for $i = \{1, 2, 3\}$ is the output defined in (15). Notably, the derivatives in this paper are calculated numerically.

Table 2
Description of the three groups of animal experiments chosen as training data sets, their characteristics, and their key features. I and H refer to insulin and glucagon, respectively.

	Exp . IDs	Weights [kg]	Bolus Types	Injections	Key Features
Group 1	#02	36	IP	I & H	1. Different combinations of I and H boluses to excite the dynamics of Glycogen storage level. 2. Different bolus sizes and body weights.
	#04	37	IP	I & H	
	#05	40	IP	I & H	
	#06	52	IP	I & H	
	#10	43	IP	I & H	
	#15	50	IP	I	
Group 2	#07	48	IP	I & H	1. Wide range of body weight. 2. IV and IP injections. 3. Wide range of I & H bolus sizes. 4. Regular PIL and PHL measurement.
	#11	30	IV & IP	I & H	
	#12	63	IV	I & H	
	#13	40	IV & IP	I & H	
	#14	41	IV & IP	I & H	
Group 3	#22	36	IP	I	1. Wide range of I bolus sizes. 2. Constant Glucose infusion.
	#23	36	IP	I	

5.2. Bayesian information criterion

After estimating the parameters and analyzing the inter-subject parameter variability, the rest of the experiments are used to evaluate the performance of the proposed model. The Bayesian information criterion (BIC) is employed to compare the proposed model with the other available models in the literature. The BIC is defined as follows:

$$BIC = n_s \cdot \log\left(\sigma^2\right) + p_{\#} \cdot \log(n_s) \tag{25}$$

where n_s is the number of samples, σ^2 is the mean square error (MSE) of the model, and $p_{\#}$ is the number of the parameters. As the number of samples is equal for all models, The lower MSE of the model with the minimum number of parameters will result in lower BIC values. Therefore, the lower the BIC value, the better the model performance.

6. Meta-model parameter identification using the training set

Since the model is developed for control purposes, some simplifying assumptions can be made before identifying the parameters. For example, the precise concentration of insulin or glucagon in the peritoneal fluid is not a critical factor in the control algorithms; rather, the amount (mass) of insulin and glucagon in the peritoneal fluid is required. As a result, there is no need to determine the volume of peritoneal fluid; instead, a value proportional to body weight can be assumed. Therefore, we assumed that δ_4 and δ_7 are 1 ml/kg. Furthermore, δ_1 can be found based on the concentration of the IV glucose solution used in the experiment and the approximation of the blood volume in the body based on the body weight [23]. For example, in our animal trials, we utilized glucose with a 200 mg/ml concentration to simulate the meals. Furthermore, based on our observations and as mentioned in [14], we assumed that 100% of the drugs administered into the peritoneal cavity absorbs to the PV; as a result, $\delta_{12} = 100\%$ and $\delta_{14} = 100\%$. After selecting the data set and having made the assumptions above, we identified the parameters of the meta-model described in the next section.

6.1. Performance of the trained meta-model

Table 3 presents the mean error (ME), standard deviation (SD), and mean absolute error (MAE) of the meta-model in estimating the BGL, PIL, and PHL of the selected training data. As an example, the performance of the proposed model for Pigs #4, #5, and #6 in tracking the BGL, PIL, and PHL measurements are plotted in Fig. 4. Notice that the meta-model could fit all BGL, PIL, and PHL measurements of the training data with an average MAE of 0.3 mmol/l, 2.9 mU/l, and 23 pmol/l, respectively.

The PIL and PHL measurements often contain more noise and disturbances compared to BGL due to the measurement method and endogenous secretions.

6.2. Identifiability of the model

The models (14b) and (14a) are considered locally structurally identifiable using the assumptions and the available data sets. The identifiability tests are presented in Appendix A.

6.3. Inter-subject parameter variability

The inter-subject parameter variability is investigated in this Section in order to find the individual parameters that can be classified as constant across the animals for IP injections. In the proposed meta-model, there are seventeen analogous parameters $(\beta_1, \ldots, \beta_{17})$ and one individual parameter (α_7) for IP insulin and IP glucagon injections. Using the definitions of coefficient variability and sensitivity of the outputs to parameters given in (23) and (24), the $|CV_p \cdot S_p^{y_i}|$ for the analogous parameters and for $i = \{1, 2, 3\}$ are shown in Fig. 5. Notably, the violin plots in panel (d) of Fig. 5 shows the $\%CV$ of the parameters related to body weight where $\nu_b \triangleq \omega/\delta_1$). Using Fig. 5, the variability of the parameters is discussed in three sections as follows (where they are divided based on categories shown in Fig. 5).

6.3.1. Individual parameters related to blood glucose level

To every new animal experiments, the parameter set $\{\beta_1, \beta_2, \ldots, \beta_{11}, \alpha_7\}$ is required to be identified. As shown in Fig. 5, the values of $|CV \cdot S_p^{y_1}|$ for 7 out of 12 parameters are negligible compared to the others. Therefore, they can be assumed as fixed parameters among the animals. The other five parameters are β_1, β_2, β_3, β_4, and α_7, which refer to insulin-independent glucose uptake rate, e.g., brain glucose uptake, the sensitivity of the liver to insulin, sensitivity of extra-hepatic organs to insulin, sensitivity of the body to glucagon, and the initial state of glycogen storage level. As a result, instead of identifying all 12 parameters, one needs to identify these five for each new individual. To examine this, we will re-identify only these five parameters while treating the other seven as fixed parameters for all the training and test data. It is worth mentioning that the parameters β_6 and β_7 are the parameters of the HFP effect on insulin, and they are present both in the BGL sub-model and PIL sub-models (both panels of (a) and (b) of Fig. 5).

6.3.2. Individual parameters of the PIL and PHL sub-models

Among the remaining eight parameters describing the concentration of insulin and glucagon in plasma after IP injections, $\{\beta_{15}, \beta_{16}, \beta_{17}\}$ are found to be constant across the animals since they have small $|CV \cdot S_p^{y_i}|$ for $i = \{2, 3\}$ compared to the other parameters. Notably, β_6 and β_7 are shared parameters between PIL and BGL sub-models, which are already discussed in the previous section and considered as constant parameters.

Recall that the main aim of this paper was to design the BGL model with fewer parameters, and the BGL sub-model does not include $\{\beta_{12}, \beta_{13}, \ldots, \beta_{17}\}$ in its parameters. Therefore, for every

Table 3
Mean error (ME), error standard deviation (SD), and mean absolute error (MAE) of the proposed meta-model in tracking the BGL, PIL, and PHL measurements of the training data set. Example graphs for Pigs #4–6 are shown in Fig. 4.

BGL Sub-Model (mmol/l)	Exp. ID	Pig #2	Pig #4	Pig #5	Pig #6	Pig #10	Pig #15	Pig #22	Pig #23
	ME ± SD	0.0 ± 0.5	0.0 ± 0.5	0.0 ± 0.5	0.0 ± 0.8	0.0 ± 0.3	0.0 ± 0.4	0.2 ± 0.4	0.0 ± 0.1
	MAE	0.4	0.3	0.4	0.6	0.2	0.2	0.3	0.1
	W [kg]	36	37	40	52	43	50	36	36
PIL Sub-Model (mU/l)	Exp. ID	Pig #4	Pig #5	Pig #6	Pig #11	Pig #12	Pig #13	Pig #22	Pig #23
	ME ± SD	-0.8 ± 2.9	0.0 ± 2.4	0.0 ± 4.5	-1.6 ± 4.6	-1.6 ± 10.4	-0.5 ± 3.5	0.8 ± 4.0	0.2 ± 1.2
	MAE	2.0	1.7	3.2	4.0	6.8	2.5	2.5	0.7
	W [kg]	37	40	52	30	63	40	36	36
PHL Sub-Model (pmol/l)	Exp. ID	Pig #4	Pig #5	Pig #6	Pig #7	Pig #11	Pig #12	Pig #13	Pig #14
	ME ± SD	-3 ± 12	-3 ± 9	-4 ± 17	-4 ± 9	-20 ± 31	-21 ± 82	-15 ± 52	-8 ± 40
	MAE	8	7	11	6	27	57	38	26
	W [kg]	37	40	52	48	30	63	40	41

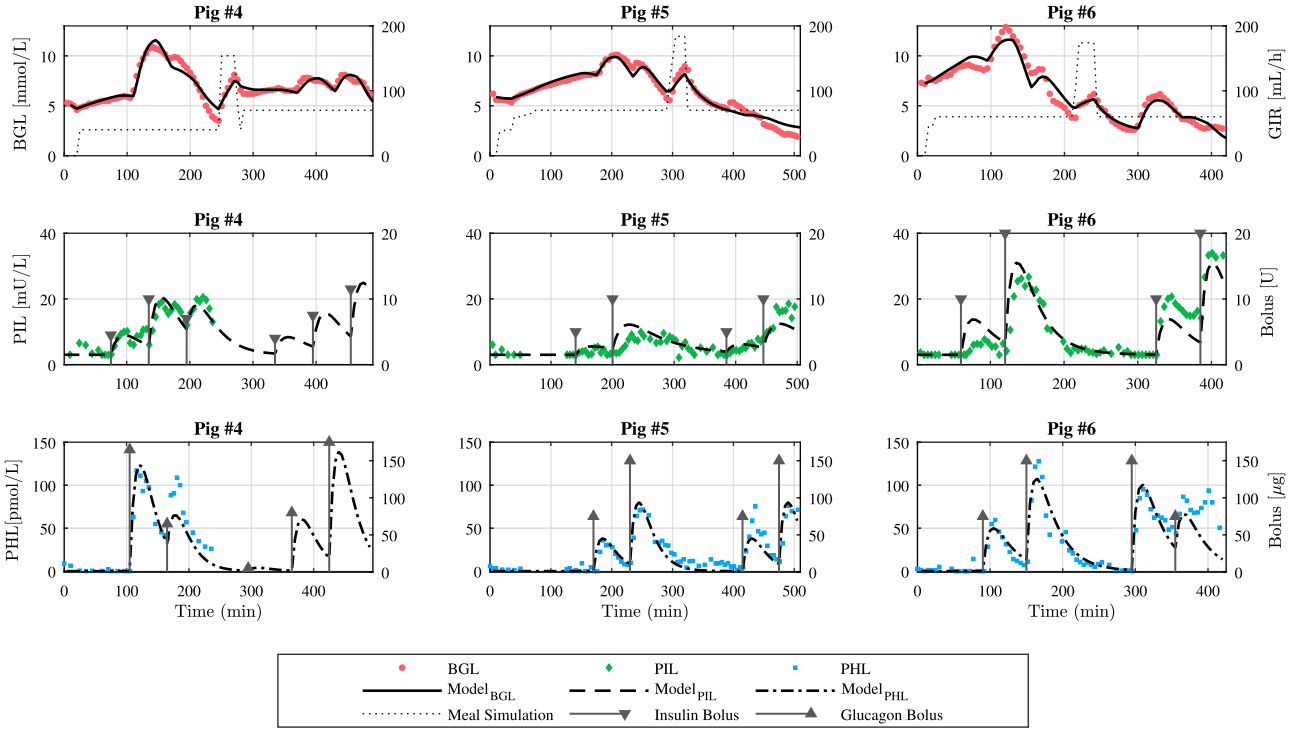

Fig. 4. As an example, the figures demonstrate how the proposed meta-model tracked blood glucose levels (BGL), plasma insulin levels (PIL), and plasma glucagon levels (PHL) in three experiments. The three trials shown here are part of the training data utilized to identify the parameters. The performance of the model on the other training data is presented in Table 3. The dashed line in the first row is the Intravenous glucose infusion rate, simulating the meal absolution rate in the intestines.

new pig, one needs to identify only five parameters $\{\beta_1, \beta_2, \beta_3, \beta_4, \alpha_7\}$. The other parameters are either constant across animals or are body weight-related parameters that can be identified using the previous experiments. Moreover, if one needs to model the PIL and PHL, then $\{\beta_{12}, \beta_{13}, \beta_{14}\}$ must be identified.

6.3.3. Weight-dependent parameters

Violin plots show the values of the *CV%* for the weight-dependent parameters in Fig. 5. ω is the body weight of the pigs, and v_b is proportional to blood volume, which directly relates to weight.

γ_1 and γ_2 are insulin and glucagon diffusion rates from the peritoneal cavity to surrounding capillaries. As expected, these parameters are identified to be inversely correlated to weight. The physical explanation may include anatomical features related to size and age, such as thicker peritoneal lining and a lower density of capillaries in the peritoneal lining in heavier animals. Notice that $\gamma_1 \in [0.54, 1.73]$ and $\gamma_2 \in [2.00, 3.62]$ which indicates that glucagon diffuses faster than insulin.

γ_3 and γ_4 are glycogen storage charging and discharging rates, respectively. In the training data, γ_3 is close to zero, indicating that the glycogen storage is being charged very slowly. Notably, it is also observed in the experiments that the pigs were responding poorly to glucagon after receiving multiple injections and at the end of experiments. This could be due to a low glucose infusion rate in our 8-hour experiments or the effect of the anesthesia, all of which cause glycogen storage to discharge faster than charging. Since one may experience a faster glycogen refill in humans or awake animal experiments, γ_3 was not omitted even if it was close to zero in these experiments.

The value of γ_4 has been shown to be inversely related to body weight in the identification, implying that heavier subjects have bigger glycogen storage and can release more glucose than lighter animals.

7. Performance of the training and testing of the meta-model

In the previous section, the parameters of the meta-model are identified using the training data set, and it is discovered that for every new experiment, one needs to identify only five individual parameters $(\beta_1, \ldots, \beta_4, \alpha_7)$. The other individual parameters

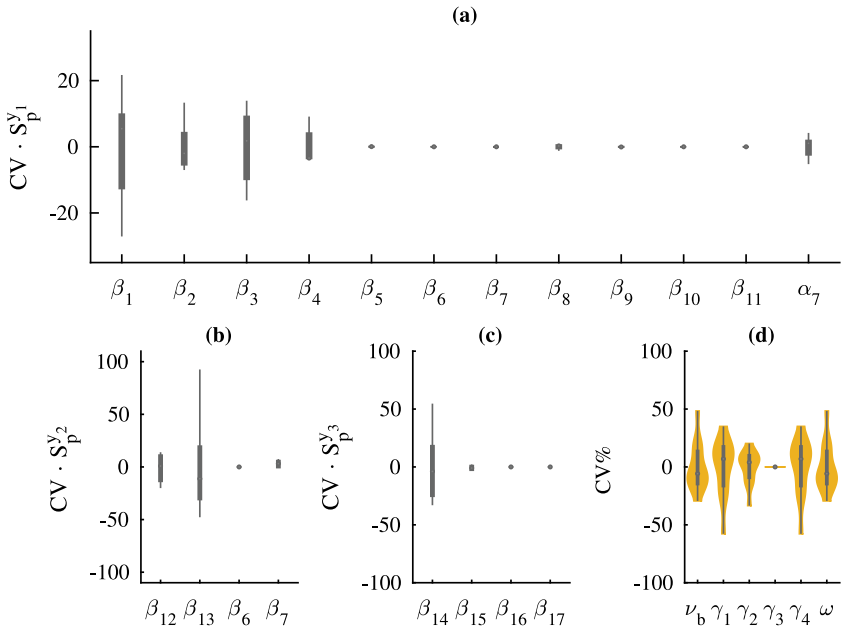

Fig. 5. The box-plot (a) shows the $CV \cdot S_p^{y_1}$ for the individual parameters that are included in the subsystem of the BGL. Panels (b) and (c) show $CV \cdot S_p^{y_1}$ and $CV \cdot S_p^{y_2}$ of the parameters that have an influence on the PIL and PHL outputs, respectively. The violin plot (d) shows the $CV\%$ of the weight-related parameters, and their variation depends on the body weight.

$(\beta_5, \ldots, \beta_{11})$ are shown to have negligible variation from subject to subject.

In this section, parameter set $\{\beta_5, \ldots, \beta_{11}\}$ are considered constant among animals and set to the mean value of identified values for the training data in the previous section. Then, the performance of the meta-model is compared with the models in the literature using the training and test data.

There are two important models in the literature; the bi-hormonal low-order model by Zazueta et al. [12] and the single-hormonal linear model by Chakrabarty et al. [25]. Therefore, we split our analysis into bi-hormonal and single-hormonal experiments when comparing the models. In addition, the classical least square method in parameter identification of all three models is used to have a fair comparison. In these identifications, the parameters of the models are identified separately for each experiment using their BGL measurements. in more detail; the following cost function is used for parameter identification of the models:

$$J_{LS}(\Psi_M) = \sum_{i=1}^{N} P_{LS}(BGL_i - M_i(\Psi_M))^2 \tag{26}$$

Where P_{LS} is a constant positive number, BGL_i is the BGL at the sample i, and M_i is the model (Meta-model, low-order, or Linear model) output for the corresponding sampling time. N denotes the number of samples in the experiment. In this cost function, the decision variables are each model's parameter set (Ψ_M). Notably, the low-order model has ten parameters (six without the glucagon sub-model), and the linear model has five parameters to identify.

The number of parameters for the meta-model is five. However, frequent blood samples from the jugular vein are taken during the bi-hormonal experiments in bi-hormonal experiments for PIL and PHL measurements. As a result, blood volume is no longer solely dependent on body weight and may be influenced by the number of samples taken. Two meta-models are considered to make up for it: meta-model 1 and meta-model 2, with δ_7 being treated as a fixed and individual parameter, respectively.

The performance of meta-model 1 and meta-model 2 are compared to the other models in Table 4. Meta-model 1 and meta-model 2 have similar performance in training and test data. One can conclude that the parameters of the model are identified correctly using the training data set. By looking at the Average values of the errors from different models, one can conclude that all the models have acceptable performance for control purposes, and no significant differences can be found between the models. However, the proposed meta-model 1 and meta-model 2 require fewer parameters to be identified than the other models in the literature.

The BGL, PIL, and PHL measurements from Pigs #01, 09, and 16 versus the meta-model 2 (for Pig#01, and 09) and meta-model 1 (for Pig #15) responses are shown in Fig. 6. Among the test data, Pig #1 and #9 have the inputs with the most excitation inputs, e.g., a wide range of insulin, glucagon, and glucose infusions. Therefore, one can conclude that the proposed meta-model can simulate the behavior of glucose metabolism of various body weights in both complex and simple scenarios.

7.1. Summary of training and testing the meta-model

In the previous sections, the parameters of the meta-model are identified using the selected training data. The primary goal of this approach is to identify parameters that are not identifiable when the BGL is the only available data. This is accomplished by utilizing prior data from other animals for whom the PIL and PHL are measured.

The variability of the individual parameters among the different animals is discussed. It is demonstrated that one must identify only $\{\beta_1, \ldots, \beta_4, \alpha_7\}$ for every new experiment. The rest of the parameters are fixed parameters or weight-related parameters obtained from prior information.

Moreover, It is shown that the proposed meta-model can fit the BGL measured from pigs and provide similar performance with fewer parameters compared to the available models in the literature. One can conclude that the identification procedure of the trained meta-model is easier and faster than the other models.

In the following sections, the predicting performance of the meta-model is evaluated and compared with the other models in two different practical scenarios.

Table 4
The mean error (ME), standard deviation (SD), mean absolute error (MAE) [mmol/l], and the Bayesian information criterion (BIC) for different models and experiments. In the case of bi-hormonal experiments, two versions of the meta-model were analyzed, meta-model 1, and meta-model 2, when considering ν as an individual parameter (to compensate for the volume of the blood taken for BGL, PIL, and PHL analysis). For the single-hormonal experiments, only meta-model 1 is used since there were fewer blood samples taken from them. Notably, the parameters of the BGL sub-model for single-hormonal experiments are not taken into account. Notably, results for Pigs #12–#14 are not presented since they contain IV insulin and glucagon infusions from the beginning of the experiment. However, for Pig #11, the IV infusions were given at the end of the experiment, and the performances of the different models are presented for the IP infusion parts.

	Model:	Meta-Model1					Low-Order Model [14]					Meta-Model2				
Number Of Parameter:		5					10					6				
	Exp. ID	ME	±	SD	MAE	BIC	ME	±	SD	MAE	BIC	ME	±	SD	MAE	BIC
Insulin & Glucagon Injections (IP)	Pig #01	0.00	±	0.37	0.30	-187	0.02	±	0.28	0.23	-228	0.02	±	0.29	0.24	-242
	Pig #02(1)	0.00	±	0.50	0.40	-110	0.01	±	0.74	0.55	-14	0.00	±	0.50	0.37	-112
	Pig #03	0.04	±	0.55	0.40	-86	0.00	±	0.24	0.19	-219	0.05	±	0.45	0.38	-120
	Pig #04(1,2,3)	0.01	±	0.50	0.30	-123	0.01	±	0.41	0.32	-130	0.05	±	0.47	0.35	-123
	Pig #05(1,2,3)	0.05	±	0.43	0.30	-148	0.07	±	0.48	0.43	-101	0.05	±	0.43	0.31	-179
	Pig #06(1,2,3)	0.04	±	0.71	0.54	-36	0.09	±	0.77	0.59	1	0.05	±	0.71	0.54	-37
	Pig #07(1,2,3)	0.00	±	1.48	0.97	103	0.09	±	0.73	0.51	-18	0.05	±	1.46	0.95	100
	Pig #08	0.07	±	0.80	0.65	-18	0.05	±	0.49	0.37	-92	0.05	±	0.80	0.64	-19
	Pig #09	0.04	±	0.74	0.54	-31	0.04	±	0.54	0.40	-64	0.05	±	0.63	0.49	-59
	Pig #10(1)	0.01	±	0.27	0.23	-191	0.00	±	0.27	0.22	-175	0.05	±	0.28	0.23	-192
	Pig #11(2,3)	0.02	±	0.50	0.41	-77	0.12	±	1.11	0.85	57	0.05	±	0.47	0.39	-87
Average	Training Data	**0.02**	±	**0.63**	**0.47**	**-81**	-	±	-	-	-	**0.04**	±	**0.54**	**0.44**	**-110**
	Test Data	**0.04**	±	**0.62**	**0.45**	**-83**	-	±	-	-	-	**0.04**	±	**0.62**	**0.45**	**-90**
	All Data	**0.03**	±	**0.62**	**0.46**	**-82**	**0.05**	±	**0.55**	**0.42**	**-89**	**0.04**	±	**0.59**	**0.44**	**-97**
	Model:	Meta-Model1					Low-Order Model					Linear Model [28]				
Number Of Parameter:		3					6					5				
	Exp. ID	ME	±	SD	MAE	BIC	ME	±	SD	MAE	BIC	ME	±	SD	MAE	BIC
Only Insulin Injections (IP)	Pig #15(1)	0.06	±	0.41	0.26	-77	0.06	±	0.38	0.23	-71	0.00	±	1.00	0.69	19
	Pig #16	0.04	±	0.23	0.17	-210	0.04	±	0.39	0.30	-118	0.00	±	0.26	0.20	-182
	Pig #17	0.07	±	0.69	0.50	-55	0.02	±	0.38	0.26	-143	0.02	±	0.45	0.26	-111
	Pig #18	0.06	±	0.53	0.43	-94	0.01	±	0.43	0.36	-116	0.01	±	0.48	0.34	-101
	Pig #22(1,2)	0.01	±	0.38	0.33	-155	0.02	±	0.40	0.34	-140	0.00	±	0.38	0.29	-151
	Pig #23(1,2)	0.01	±	0.15	0.49	-336	0.01	±	0.16	0.13	-307	0.00	±	0.37	0.29	-160
	Pig #24	0.05	±	0.33	0.24	-192	0.07	±	0.33	0.22	-181	0.01	±	0.22	0.15	-267
	Pig #25	0.03	±	0.14	0.11	-354	0.00	±	0.10	0.07	-417	0.00	±	0.16	0.12	-329
	Pig #26	0.06	±	0.35	0.32	-182	0.01	±	0.22	0.17	-282	0.00	±	0.35	0.30	-188
	Pig #27	0.04	±	0.30	0.27	-209	0.01	±	0.25	0.21	-229	0.00	±	0.26	0.22	-226
	Pig #28	0.02	±	0.28	0.23	-220	0.01	±	0.12	0.10	-362	0.00	±	0.08	0.05	-456
	Pig #29	0.06	±	0.47	0.39	-128	0.05	±	0.46	0.38	-116	0.00	±	0.30	0.25	-204
	Training Data	0.08	±	0.94	0.36	-147	-	±	-	-	-	-	±	-	-	-
	Test Data	**0.05**	±	**0.37**	**0.30**	**-194**	-	±	-	-	-	-	±	-	-	-
	All Data	**0.04**	±	**0.36**	**0.31**	**-184**	**0.03**	±	**0.30**	**0.23**	**-207**	**0.00**	±	**0.36**	**0.26**	**-196**

(1) BGL measurement is utilized in training the Meta-model.
(2) PIL measurement is utilized in training the Meta-model.
(3) PHL measurement is utilized in training the Meta-model.

8. Performance of the meta-model in predicting the BGL

The combination of MPC with moving horizon estimation (MHE) is one of the most commonly used control approaches in APs [26]. The MHE uses the historical BGL data to estimate state values. Based on the estimated states, the MPC predicts the BGL and finds optimal insulin or glucagon boluses to keep the BGL in the range. As a result, the proposed model should be consistent with past data and effective at predicting.

In this section, we compare the performance of the proposed meta-model (in which $\{\beta_1, \ldots, \beta_4, \alpha_7\}$ must be identified) with the other models in terms of prediction. For that purpose, we proposed the following two scenarios:

8.1. Scenarios 1: Bi-hormonal model identification and prediction at every sampling time

This scenario aims to evaluate the proposed meta-model and low-order model fitting the data and predicting each sampling time for bi-hormonal experiments.

The parameters are re-identified for both models after measuring the BGL at every sampling time. Then, based on the identified model and future inputs, a 100 min prediction will be performed. After that, the MSE of the models for both fitting to the measured BGL and the prediction are calculated. For example, at ith sample, the fitting MSE is the mean squared error of the model in fitting to the BGL samples $\{1, \ldots, i\}$, and Prediction MSE is the mean squared error of the model in predicting the BGL samples $\{i+1, \ldots, (i+100/T_s)\}$.

In order to have proper initial values for the parameter estimation, one needs to have at least one insulin and one glucagon infusion before starting the identification and predictions. Therefore, this scenario starts after collecting 100 min of the BGL measurements, and the starting model is obtained by the parameter identification over that 100 min time window. Notably, the half-life IP insulin (for the kind of insulin used in our tests) is within the first 100 min of injection, according to our experience. Additionally, glucagon effects fade off after 100 min. Therefore, the 100 min prediction window for IP insulin and glucagon is chosen in this scenario.

To have a fair comparison of the models, an overview of the fitting MSE and prediction MSE are shown in Fig. 7 for the experiments Pig#{1, 3, 8, 16, 17, 18, 24, 25, 26, 27, 28, 29}. The selected experiments contain only IP insulin and glucagon with continuous IV glucose infusion that was not used to train the meta-model. Pig#9 was not included since the glucose infusion in this experiment was discontinuous and unrealistic for real-life situations. The supplementary material in Appendix B provides the detailed performance of each model in Scenario 1 on all available experiments with IP injections.

As shown in Fig. 7, the low-order model has a mean model fitting MSE that is 26.6% lower than the meta-model. For both models, the mean fitting MSE is less than 1 $[\text{mmol/l}]^2$. In prediction, the meta-model has a 39.2% lower mean MSE and a 64.0% lower standard deviation than that of the low-order model. The meta model has a mean prediction MSE of less than 1 $[\text{mmol/l}]^2$.

In summary, by comparing the performance of the models in scenario 1, one can infer that the low-order model performs better in fitting the measurements. However, the fitting MSE of

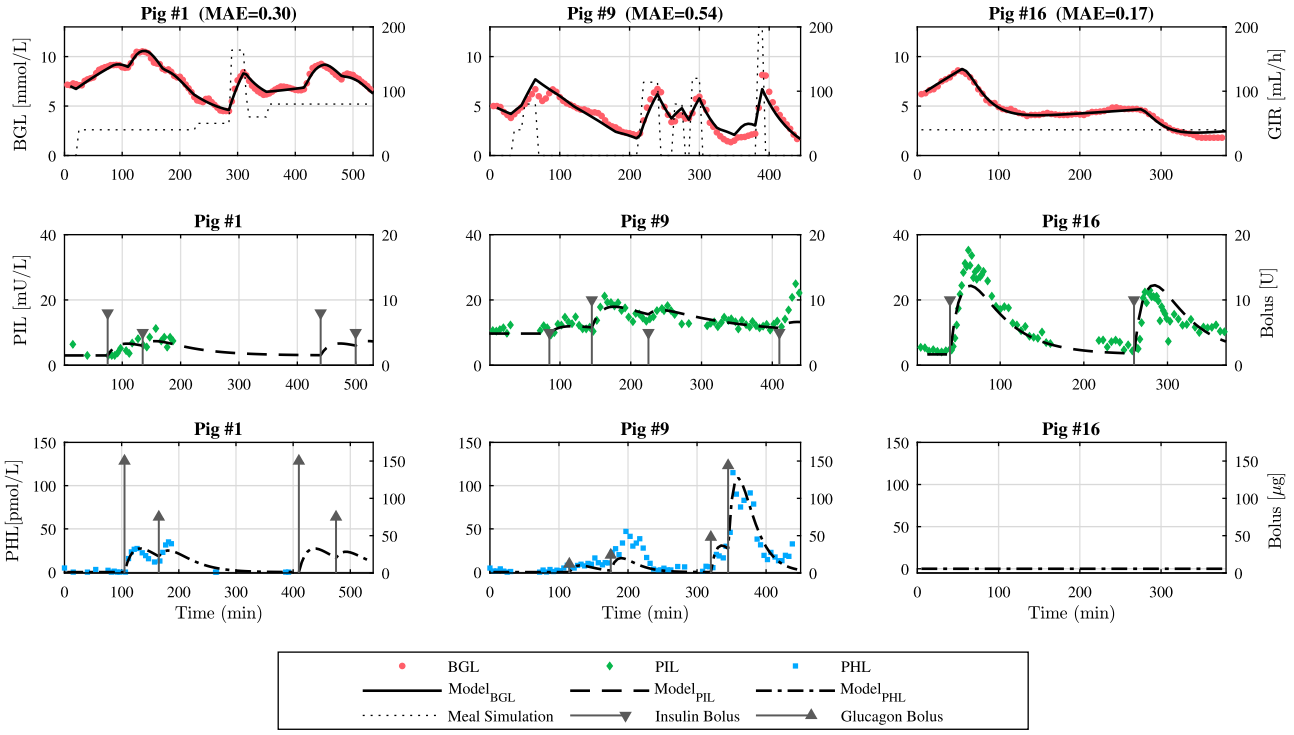

Fig. 6. Three examples of meta-model performance on test data are shown in the figure. Notably, meta-model 1 is used for single-hormonal experiment Pig #16 and meta-model 2 is utilized for bi-hormonal experiments in Pigs #01, #09. The performance of the presented model in fitting to the BGL measurements for the other experiments is presented in Table 4. However, the MAE (mean absolute error) of the proposed model is for the BGL measurements written in the titles in order to quantify the quality of the fittings. The dashed line in the first row is the IV glucose infusion rate which simulates the meal digestion rate in the intestines.

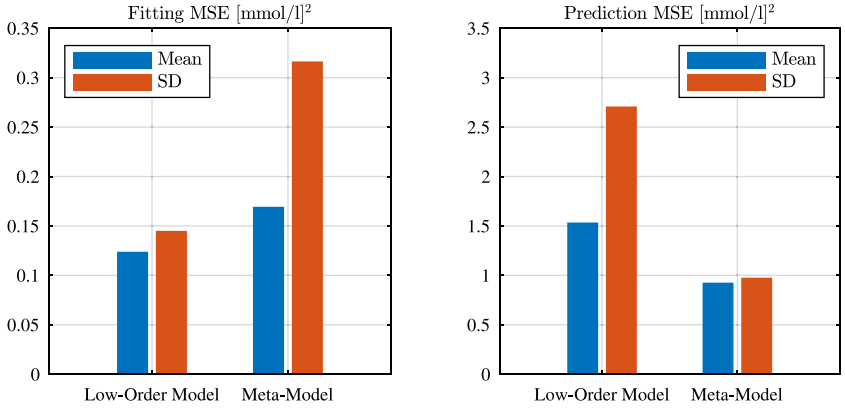

Fig. 7. The figure compares the proposed meta-model with the low-order model regarding the fitting MSE and prediction MSE for the selected test experiments in Scenario 1. The panel on the left shows the mean and standard deviation (SD) of fitting MSE at all sampling times of the selected experiments. Similarly, the panel on the right shows the mean and SD of 100 min of prediction MSE at all sampling times for the selected experiments.

both models is in the acceptable range for control purposes. In contrast, the proposed meta-model performs significantly better in prediction, which is more important than fitting when you aim to use the model in control. In summary, the fewer parameters, the acceptable fitting MSE, and the low prediction MSE in the meta-model make it a suitable choice for model-based control.

8.1.1. Scenarios 2: Prediction of the BGL interaction with different insulin boluses

This scenario investigates the effect of considering the HFP effect on prediction and fitting to the measurements. Among the available animal experiments, Pigs #23–28 with weights of 36–41 kg were given a constant basal glucose infusion proportional to their weight and three different insulin boluses, i.e., 2, 5, and 10 Units with various orders. These experiments are performed to investigate the saturation of the HFP published in [11]. It is shown that the liver of these subjects is saturated after 5U of insulin, and then the insulin enters the central blood circulation. The duration of the experiment chosen for this scenario is about 500 min in which insulin boluses were given approximately at $t_1 = 75$, $t_2 = 210$, and $t_3 = 350$ min.

In this scenario, we first identified the parameters of the different models using the BGL measurements in the time interval $[0, t_2)$ and evaluated the models' prediction performance in the time interval $[t_2, 480)$. Then, we identified the parameters using the BGL measurements interval $[0, t_3)$ and again evaluated the prediction performance during the time interval $[t_3, 480)$. Both identification and prediction MSE of each experiment for the different models are presented in Table 5. Please Note that the Pig #23 was included in the training data while it is also included

Table 5
Mean squared error (MSE) of the different models in identification and prediction for the second scenario. The terms *Iden.* and *Pred.* in this table relate to the identification and prediction MSEs, respectively.

Identification Period	Model	Pig #23		Pig #24		Pig #25		Pig #26		Pig #27		Pig #28		Average	
		Iden.	Pre.	Iden.	Pre.	Iden.	Pre.	Iden.	Pre.	Iden.	Pre.	Iden.	Pre.	Iden.	Pre.
$[0, t_2)$	Linear Model	0.0	0.5	0.1	0.2	0.0	1.8	0.0	26.6	0.1	1.6	0.0	13.7	**0.0**	**7.4**
	Low-order Model	0.0	2.6	0.1	10.6	0.0	0.6	0.0	11.8	0.0	1.3	0.0	1.1	**0.0**	**4.7**
	Meta-Model	0.0	0.2	0.1	0.8	0.0	0.6	0.0	1.0	0.1	0.2	0.0	0.6	**0.0**	**0.6**
$[0, t_3)$	Linear Model	0.1	3.7	0.1	0.4	0.0	0.8	0.1	8.1	0.1	1.7	0.0	0.0	**0.1**	**2.5**
	Low-order Model	0.0	3.9	0.1	0.6	0.0	0.0	0.0	0.8	0.1	2.5	0.0	0.2	**0.0**	**1.3**
	Meta-Model	0.0	0.1	0.1	1.0	0.0	0.1	0.1	0.5	0.1	0.5	0.0	0.4	**0.1**	**0.4**

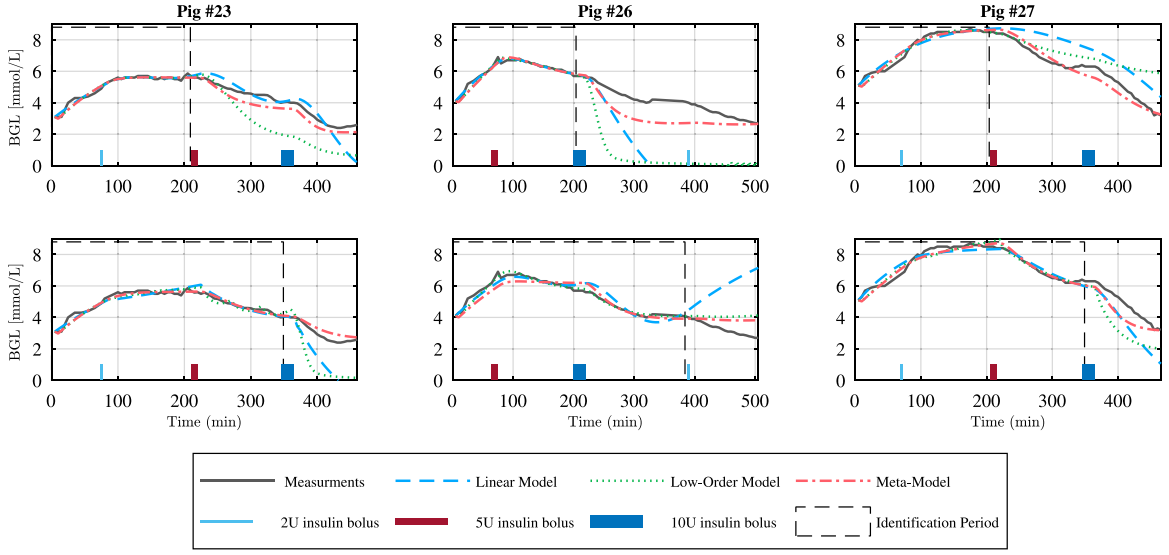

Fig. 8. Comparison of different models' prediction performance. The identification period for the upper figures was $t_2 = 200$ min and $t_3 = 350$ min for the lower figures. The proposed meta-model has a better prediction for both small and large insulin boluses; this is most notable for the 10U insulin bolus because it is the only model considering the HFP effect. In contrast, the other models fail to respond to smaller and larger insulin boluses.

in this scenario to compare the performance of the meta-model on both training and test data.

The proposed meta-model outperformed the other models' predictions when different insulin boluses were given. As an example, the performance of the models in fitting and predicting the BGL measurement of Pigs #23, #26, and #27 are shown in Fig. 8. Due to the modeled HFP effect and the prior information in the meta-model, it performs better in response to 5 and 10U, while the other models fail to predict the BGL correctly.

By looking at the average error of the models in Fig. 7 and Table 5, one can conclude that the proposed meta-model and the models in the literature for the IP route can track the BGL measurements for anesthetized pigs with acceptable performance. However, the proposed meta-model outperforms the other models in terms of prediction. The average prediction MSE in Table 5 shows that the low-order model performs better than the linear model. Additionally, because of fewer parameters of the meta-model, this model can be set up and used in the controller more quickly than the other models.

9. Discussions

In contrast to the SC drug pathway, it is demonstrated in [5] that the insulin absorption from the peritoneal cavity is quick enough to control the BGL without the meal announcement. Furthermore, an important feature of IP injection is the fact that insulin is transported directly to the liver through the PV, where the HFP effect applies before entering the central blood circulation system. It is shown that the HFP effect significantly influences how the body responds to different insulin bolus sizes. For that reason, a nonlinear model containing the HFP effect is presented.

In order to identify the parameters of the designed model, a large number of tests must be performed to stimulate all the system dynamics. Furthermore, it is necessary to measure both the PIL and PHL to address the identifiability issues for this model. However, invasive tests and measurements are not applicable at a large scale or are dangerous for the animals.

As an alternative to performing all the tests on each subject, the meta-model is designed to allow us to perform the tests on a large group of animals. This approach allows us to conduct less invasive experiments and identify parameters that are weight-dependent or parameters that have a fixed value for all animals.

Using the training data, it is shown that only five parameters must be individually identified for each animal to simulate the BGL dynamics. The remaining parameters are either constant among the animals or can be calculated using body weight.

The model is identified using data and assumptions related to anesthetized pigs weighing between 30 kg and 60 kg. It is shown that the model has an acceptable performance. In addition, it performs accurately in predicting the BGL for various inputs and provides better prediction with fewer parameters, making it ideal for control purposes. In future work, one might design the MPC controller for APs using the model proposed in this paper.

The same procedure used in this paper can also be used for humans. However, some distinctions between the IP structures of humans and pigs must be taken into account. In addition, one can use the proposed meta-model to design less invasive experiments for humans or awake animals.

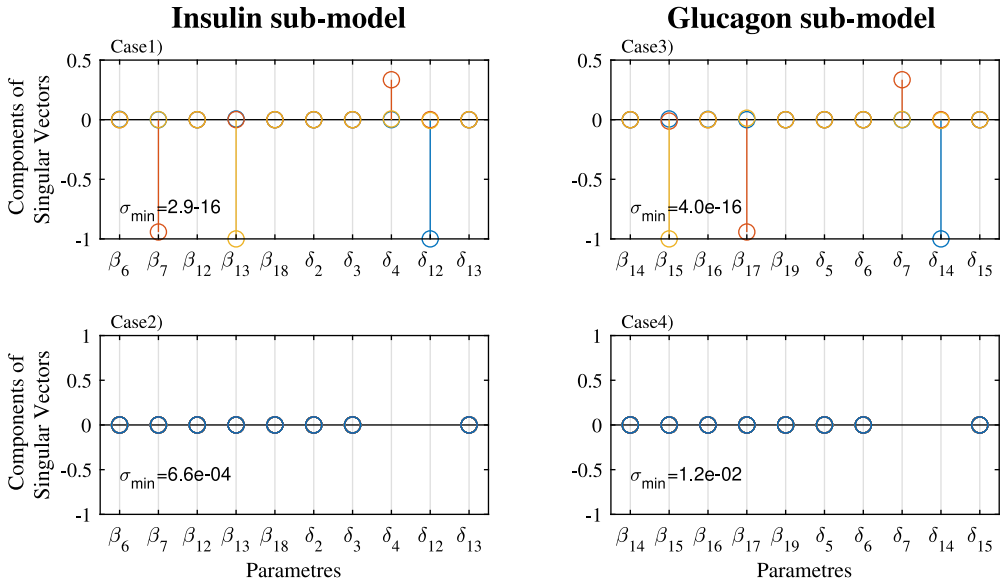

Fig. A.9. Components of the columns of V^i that $S_r(t, \eta^i)$ has eigenvalues less than 10^{-6} for system (14a). The non-zero (non-vanishing) components are associated with the null space of $S_r(t, \eta^i)$ as described in Appendix A. Case 1 and case 3 are the identification based on PIL and PHL measurements of all training data. Case 2 and case 4 are with assuming $\delta_4, \delta_7, \delta_{12}$ and δ_{14} equal to one (as explained in Section 6). There are no non-vanishing components in case 2 and case 4. The smallest singular value is printed in the lower-left corner.

Due to limitations with experiments in anesthetized animals, the length of the experiments was shorter than a half-day. Therefore, we assumed that the parameters remained constant throughout the experiments. One might need to consider intra-subject variation in extended experiments or human experiments. In addition, one may need more training data for longer experiments. However, the thirteen training experiments for this paper seem to be enough to identify the parameters of the meta-model.

CRediT authorship contribution statement

Karim Davari Benam: Conceptualization, Mathematical design, Simulations. **Hasti Khoshamadi:** Data curation, Writing – original draft. **Marte Kierulf Åm:** Data curation, Writing – original draft. **Øyvind Stavdahl:** Supervisor. **Sebastien Gros:** Conceptualization, Mathematical design, Supervisor. **Anders Lyngvi Fougner:** Conceptualization, Mathematical design, Supervisor.

Declaration of competing interest

The authors declare that they have no known competing financial interests or personal relationships that could have appeared to influence the work reported in this paper.

Data availability

The data that has been used is confidential.

Acknowledgments

The animal experiments were performed at the Comparative Medicine Core Facility (CoMed) at the Norwegian University of Science and Technology (NTNU). CoMed is funded by the Faculty of Medicine and Health Sciences at NTNU and the Central Norway Regional Health Authority. This research is also funded by the Research Council of Norway (project no. 248872 and 294828) and the Centre for Digital Life Norway. We would like to thank Oddveig Lyng, Patrick Christian Bösch, and Ilze Dirnena-Fusini for their invaluable contribution to the data collection. We also thank Professor Sven Magnus Carlsen for his help in designing experiments and discussions.

Appendix A. Local structural identifiability of the parameters

In this part, we examine the identifiability of the proposed meta-model. To this end, we employ the algorithm described in [27]. In this algorithm, the sensitivity matrix $S_r(t, \eta)$ defined in (A.1), which is the sensitivity of the output of the model, y, at each sampling time, $t = \{t_o, \ldots, t_n\}$, to the parameters, $\eta = \{\eta_1, \ldots, \eta_p\}$, must be found locally around the identified values for the parameters.

$$S_r(t, \eta) = \begin{pmatrix} \frac{\eta_1}{y(t_0)}\frac{\partial y(t_0)}{\partial \eta_1} & \cdots & \frac{\eta_p}{y(t_0)}\frac{\partial y(t_0)}{\partial \eta_p} \\ \vdots & \vdots & \vdots \\ \frac{\eta_1}{y(t_N)}\frac{\partial y(t_N)}{\partial \eta_1} & \cdots & \frac{\eta_p}{y(t_N)}\frac{\partial y(t_N)}{\partial \eta_p} \end{pmatrix} \tag{A.1}$$

By considering small random perturbations in parameters sets, η^i, one needs to calculate singular value decomposition (SVD) for $S_r(t, \eta^i)$ as follows:

$$S_r\left(t, \eta^i\right) = U_i \Sigma_i V_i^T \tag{A.2}$$

where U_i and V_i are orthogonal matrices, and Σ_i is a matrix containing the p singular values of $S_r(t, \eta^i)$ in decreasing order on the diagonal, while all the other elements are zero. It is shown that in [27] that if the smallest singular value of Σ_i is zero or very small, the last column of V_i shows the parameters that are correlated and non-identifiable. Notable, due to numerical errors, we considered any singular values less than 10^{-6} as zero. Therefore, the columns of V_i related to any singular values less than 10^{-6} will be considered null space.

This algorithm is used in four stages to evaluate the effectiveness of the proposed meta-model and assumptions in reducing the number of non-identifiable parameters:

A.1. Identifiability of the meta-model using single BGL measurements

This section aims at finding which of the parameters of the proposed individual model (14b) are non-identifiable without having the PIL, PHL measurements, and the multiple animal BGL data. To do this, we identified the parameters using the BGL

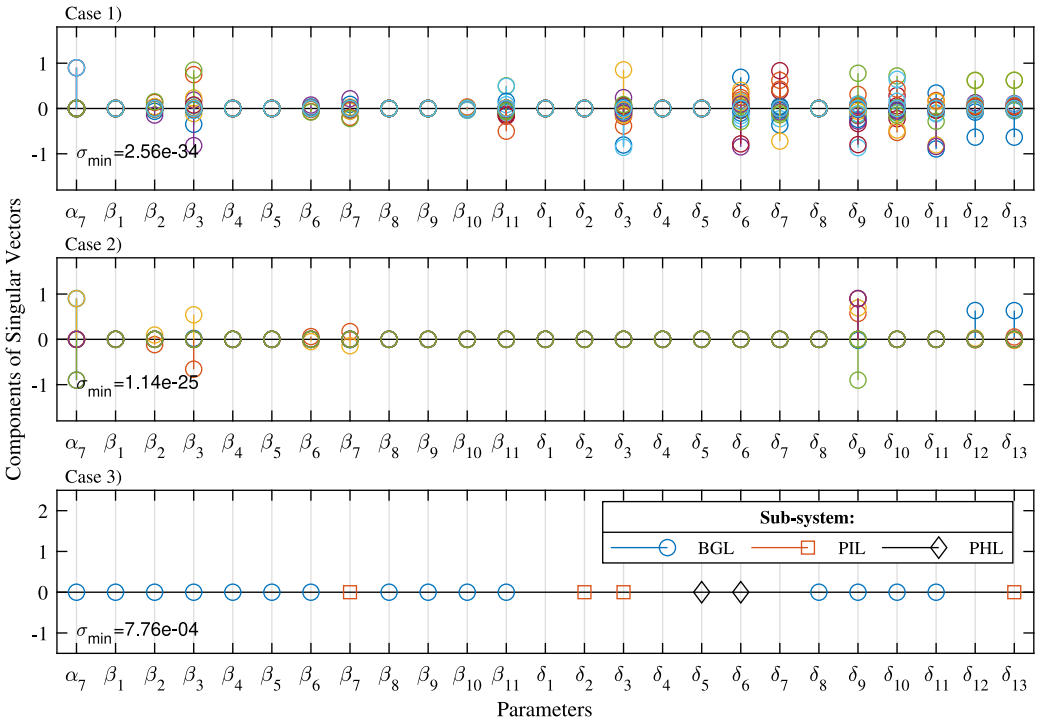

Fig. A.10. Components of the columns of V^i that $S_r(t, \eta^i)$ has eigenvalues less than 10^{-6} for system (14b). The non-zero (non-vanishing) components are associated with the null space of $S_r(t, \eta^i)$ as described in Appendix A. Case 1 is the identification based on only BGL measurements of Pig#6, Case 2 is identification based on multiple pig BGL measurements belonging to training data, and case 3 is the identification using the assumption that $\delta_4, \delta_7, \delta_{12}$ and δ_{14} are equal to one (as explained in Section 6) and taking PIL, PHL, and BGL of all training data into account. There are no non-vanishing components in case 3. The smallest singular value is printed in the lower-left corner.

measurements of Pig#6. As shown in the first case of Fig. A.10, thirteen parameters in (14b) are correlated. Notably, the reason for choosing the Pig#6 for this example is that it had received wide ranges of insulin, glucagon, and glucose infusions.

A.2. Identifiability of the meta-model using BGL measurements from multiple animals

In this stage, we investigate how many parameters become identifiable by using the BGL measurements of the eight pigs named as training data. As shown in the second case of Fig. A.10, eight parameters in (14b) are correlated in that case.

A.3. Identifiability of the PIL and PHL sub-models

By employing all of the PIL and PHL measurements of the training data in identification, four parameters are correlated in both the PIL and PHL sub-models. The correlated parameters are shown in cases 1 and 3 of Fig. A.9. However, as shown in cases 2 and 4 of Fig. A.9, with the assumptions given in Section 6 for preselecting values for $\delta_4, \delta_7, \delta_{12}$ and δ_{14}, no correlated parameters are found. Therefore, the PIL and PHL sub-models are considered structurally identifiable with the parameters found using the selected training data and the assumptions in Section 6.

A.4. Identifiability of the meta-model using the chosen training data set

For the meta-model parameters that are identified using the assumption outlined in Section 4 as well as the BGL, PIL, and PHL measurements present in the training data set, the minimum eigenvalue of the sensitivity matrix is greater than $10 - 2.94$. In other words, all the parameters of the meta-model can be considered structurally identifiable. As it is shown in the third case of Fig. A.10, there are no parameters in (14b) that are correlated in that case.

Appendix B. Supplementary data

Supplementary material related to this article can be found online at https://doi.org/10.1016/j.jprocont.2022.11.008.

References

[1] A. Katsarou, S. Gudbjörnsdottir, A. Rawshani, D. Dabelea, E. Bonifacio, B.J. Anderson, L.M. Jacobsen, D.A. Schatz, Å. Lernmark, Type 1 diabetes mellitus, Nat. Rev. Dis. Primers 3 (1) (2017) 1–17.
[2] P. Herrero, J. Bondia, N. Oliver, P. Georgiou, A coordinated control strategy for insulin and glucagon delivery in type 1 diabetes, Comput. Methods Biomech. Biomed. Eng. 20 (13) (2017) 1474–1482.
[3] S.J. Moon, I. Jung, C.-Y. Park, Current advances of artificial pancreas systems: A comprehensive review of the clinical evidence, Diabetes Metabolism J. 45 (6) (2021) 813–839.
[4] C. Cobelli, E. Renard, B. Kovatchev, Artificial pancreas: past, present, future, Diabetes 60 (11) (2011) 2672–2682.
[5] C. Toffanin, L. Magni, C. Cobelli, Artificial pancreas: In silico study shows no need of meal announcement and improved time in range of glucose with intraperitoneal vs. Subcutaneous insulin delivery, IEEE Trans. Med. Robot. Bionics 3 (2) (2021) 306–314.
[6] J.A. Nelson, R. Stephen, S.T. Landau, D.E. Wilson, F.H. Tyler, Intraperitoneal insulin administration produces a positive portal-systemic blood insulin gradient in unanesthetized, unrestrained swine, Metabolism 31 (10) (1982) 969–972.
[7] C. Botz, B. Leibel, W. Zingg, R. Gander, A. Albisser, Comparison of peripheral and portal routes of insulin infusion by a computer-controlled insulin infusion system (artificial endocrine pancreas), Diabetes 25 (8) (1976) 691–700.
[8] A. Giacca, A. Caumo, G. Galimberti, G. Petrella, M.C. Librenti, M. Scavini, G. Pozza, P. Micossi, Peritoneal and subcutaneous absorption of insulin in type I diabetic subjects, J. Clin. Endocrinol. Metab. 77 (3) (1993) 738–742.

[9] A.M. Albanese, E.F. Albanese, J.H. Miño, E. Gómez, M. Gómez, M. Zandomeni, A.B. Merlo, Peritoneal surface area: measurements of 40 structures covered by peritoneum: correlation between total peritoneal surface area and the surface calculated by formulas, Surg. Radiol. Anat. 31 (5) (2009) 369–377.
[10] M. Schiavon, C. Cobelli, C. Dalla Man, Modeling intraperitoneal insulin absorption in patients with type 1 diabetes, Metabolites 11 (9) (2021) 600.
[11] I. Dirnena-Fusini, M.K. Åm, A.L. Fougner, S.M. Carlsen, S.C. Christiansen, Intraperitoneal insulin administration in pigs: effect on circulating insulin and glucose levels, BMJ Open Diabetes Res. Care 9 (1) (2021) e001929.
[12] C. Lopez-Zazueta, A.L. Fougner, et al., Low-order nonlinear animal model of glucose dynamics for a bihormonal intraperitoneal artificial pancreas, IEEE Trans. Biomed. Eng. (2021).
[13] M.K. Åm, I. Dirnena-Fusini, A.L. Fougner, S.M. Carlsen, S.C. Christiansen, Intraperitoneal and subcutaneous glucagon delivery in anaesthetized pigs: effects on circulating glucagon and glucose levels, Sci. Rep. 10 (1) (2020) 1–8.
[14] V. Claassen, Intraperitoneal drug administration, Negl. Factors Pharmacol. Neurosci. Res. 12 (1994) 46–58.
[15] D.H. Wasserman, Four grams of glucose, Am. J. Physiol.-Endocrinol. Metab. 296 (1) (2009) E11–E21.
[16] J.E. Hall, M.E. Hall, Guyton and Hall Textbook of Medical Physiology E-Book, Elsevier Health Sciences, 2020.
[17] P. Canal, Y. Plusquellec, E. Chatelut, R. Bugat, J. De Biasi, G. Houin, A pharmacokinetic model for intraperitoneal administration of drugs: application to teniposide in humans, J. Pharm. Sci. 78 (5) (1989) 389–392.
[18] J.M. Collins, R.L. Dedrick, F.G. King, J.L. Speyer, C.E. Myers, Nonlinear pharmacokinetic models for 5-fluorouracil in man: intravenous and intraperitoneal routes, Clin. Pharmacol. Ther. 28 (2) (1980) 235–246.
[19] C. Mulder, A.J. Hendriks, Half-saturation constants in functional responses, Glob. Ecol. Conserv. 2 (2014) 161–169.
[20] V. Rudralingam, C. Footitt, B. Layton, Ascites matters, Ultrasound 25 (2) (2017) 69–79.
[21] K.P. Davy, D.R. Seals, Total blood volume in healthy young and older men, J. Appl. Physiol. 76 (5) (1994) 2059–2062.
[22] A. Raue, C. Kreutz, T. Maiwald, J. Bachmann, M. Schilling, U. Klingmüller, J. Timmer, Structural and practical identifiability analysis of partially observed dynamical models by exploiting the profile likelihood, Bioinformatics 25 (15) (2009) 1923–1929.
[23] S.L. Hansard, H. Sauberlich, C. Comar, Blood volume of swine, Proc. Soc. Exp. Biol. Med. 78 (2) (1951) 544–545.
[24] S. Wolfensohn, M. Lloyd, Handbook of Laboratory Animal Management and Welfare, John Wiley & Sons, 2008.
[25] A. Chakrabarty, J.M. Gregory, L.M. Moore, P.E. Williams, B. Farmer, A.D. Cherrington, P. Lord, B. Shelton, D. Cohen, H.C. Zisser, et al., A new animal model of insulin-glucose dynamics in the intraperitoneal space enhances closed-loop control performance, J. Process Control 76 (2019) 62–73.
[26] R. Gondhalekar, E. Dassau, F.J. Doyle, Moving-horizon-like state estimation via continuous glucose monitor feedback in MPC of an artificial pancreas for type 1 diabetes, in: 53rd IEEE Conference on Decision and Control, IEEE, 2014, pp. 310–315.
[27] J.D. Stigter, J. Molenaar, A fast algorithm to assess local structural identifiability, Automatica 58 (2015) 118–124.